THAYER SCHOOL OF ENGINEERING

DARTMOUTH COLLEGE

Hanover, New Hampshire 03755

MAGNETOPAUSE STUDIES USING DATA FROM THE ISEE MISSION (Guest Investigatorship)

FINAL TECHNICAL REPORT

NASA GRANT NSG5348

Grant Period: May 1, 1979 - Sept. 30, 1983

Prepared by

Bengt U.O. Sonnerup
Professor of Engineering
Principal Investigator

for

National Aeronautics and Space Administration

Scientific and Technical Information Facility

P.O. Box 8757 Baltimore/Washington International Airport

Maryland 21240

MAGNETOPAUSE STUDIES USING DATA FROM
THE ISEE MISSION

The scientific results of the study are described in the following publications and preprints, all of which are reproduced in this report:

1. Plasma acceleration at the earth's magnetopause: evidence for reconnection (G. Paschmann, B.U.Ö. Sonnerup, I. Papamastorakis, N. Sckopke, G. Haerendel, S.J. Bame, J.R. Asbridge, J.T. Gosling, C.T. Russell, and R.C. Elphic), Nature, 282, 243-246, 1979.

2. Theory of the low latitude boundary layer (B.U.Ö. Sonnerup). J. Geophys. Res., 85, 2017-2026, 1980.

3. Structure of the low latitude boundary layer (N. Sckopke, G. Paschmann, G. Haerendel, B.U.Ö. Sonnerup, S.J. Bame, T.G. Forbes, E.W. Hones, Jr., and C.T. Russell), J. Geophys. Res., 86, 2099-2110, 1981.

4. Evidence for magnetic field reconnection at the earth's magnetopause (B.U.Ö. Sonnerup, G. Paschmann, I. Papamastorakis, N. Sckopke, G. Haerendel, S.J. Bame, J.R. Asbridge, J.T. Gosling, and C.T. Russell), J. Geophys. Res., 86, 10049-10067, 1981.

5. Reverse draping of magnetic field lines in the boundary layer (E.W. Hones, Jr., B.U.Ö. Sonnerup, S.J. Bame, G. Paschmann, and C.T. Russell), Geophys. Res. Lett., 9, 523-526, 1982.

6. Contact discontinuities in a cold collision-free two-beam plasma (K.B. Kirkland and B.U.Ö. Sonnerup), J. Geophys. Res., 87, 10355-10362, 1982.

7. Magnetic field reconnection at the magnetopause: an overview (B.U.Ö. Sonnerup), to appear in Proceedings of Chapman Conference on Magnetic Field Reconnection, Los Alamos, N.M., October 1983; AGU Monograph Series, 1984.

8. ISEE Observations of magnetopause reconnection: the energy balance (G. Paschmann, I. Papamastorakis, N. Sckopke, B.U.Ö. Sonnerup, S.J. Bame, and C.T. Russell), to be submitted to J. Geophys. Res., 1984.

In addition, the following Master of Science theses at Dartmouth College have been supported by the grant:

9. K.B. Kirkland: An Analytical Model of Current Layers in a Collision-Free Plasma with Anisotropic Pressure, Dartmouth College, September 1980.

10. S.E. Minas: A Stability Analysis of the Interface Between the Magnetopause Boundary Layer and the Magnetosphere Including Coupling to the Ionosphere, Dartmouth College, September 1981.

11. F. Fonseca: Spectral Analysis of Magnetic Fields Around the Earth's Magnetopause, Dartmouth College, December 1983.

The results of these student research efforts are summarized in the thesis abstracts reproduced at the end of this report. Results from item (9) have been published as paper 6 above. Results from (10) and (11) have not yet been brought to a form suitable for publication.

Hanover, December 22, 1983

Bengt Sonnerup

Bengt U.Ö. Sonnerup
Professor of Engineering
Principal Investigator

MAGNETIC FIELD RECONNECTION AT THE MAGNETOPAUSE
AN OVERVIEW

B.U.Ö. Sonnerup
Thayer School of Engineering
Dartmouth College
Hanover, NH 03755

ABSTRACT

A brief summary is presented of the basic qualitative and quantitative aspects of reconnection in its magnetopause setting. First, the basic morphological and dynamic features of asymmetric reconnection are examined with emphasis on the important role played by the rotational discontinuity in these geometries. Second, the structure and other properties of rotational discontinuities are discussed. Third, the manner in which individual particles are energized or de-energized during their interaction with current layers in general, and rotational discontinuities in particular, is examined. Finally, the question of nonsteady, localized reconnection and its relation to flux transfer events is discussed and a qualitative model is proposed to describe these phenomena.

1. INTRODUCTION

Magnetic field reconnection in a plasma may in principle occur wherever the magnetic field exhibits strong shear. In planetary magnetospheres, the two principal active sites that have been considered are the magnetopause and the magnetotail. In this paper, attention is focussed on reconnection in its magnetopause setting. An overview is presented of the basic features and local signatures of the process predicted by existing theory. Important new information concerning magnetopause reconnection has been obtained during the last few years, principally as a result of the ISEE mission. These results, along with the magnetospheric consequences of magnetopause reconnection will not be dealt with in detail, since they form the topic of several papers to follow in this volume.

2. BASIC MORPHOLOGY AND DYNAMICS

In the early closed model of the magnetosphere (Johnson, 1960), the magnetopause was that surface, usually marked by an electric current sheet, which separated the earth's magnetic field from the solar-wind plasma and the interplanetary magnetic field (IMF) embedded in it. No interconnection between the two fields was included so that the magnetopause was a tangential discontinuity. When the concept of magnetic field reconnection was introduced into magnetospheric physics by Dungey (1961), the meaning of the term magnetopause became blurred. Indeed in Dungey's (1961) drawing of the open magnetosphere for purely southward IMF (Fig. 1), the magnetopause seemed to be entirely absent, except perhaps near the subsolar point. A geometry of this type would arise only if essentially all of the interplanetary magnetic flux impinging upon the magnetosphere could be reconnected.

The first quantitative analysis of the magnetopause reconnection process was carried out by Levy et al. (1964) who concluded that only some 10-20% of the incident magnetic flux would reconnect while the remainder would be carried past the magnetosphere without becoming interconnected with the earth's field. In such a situation, the effect of reconnection on the dayside magnetopause can be thought of as a small perturbation. In other words, the magnetopause remains a well defined current sheet as shown in Fig. 2. However, the physical character of this sheet changes drastically: instead of being a tangential discontinuity (TD), i.e., a layer with a vanishing normal magnetic field component, B_n, it is now a rotational discontinuity (RD) and has a small but significant B_n, amounting to 10-20% of the total field.

A rotational discontinuity is a large-amplitude Alfvén wave and the interplanetary plasma flows across it with speed equal to the Alfvén speed based on B_n. During its passage through the dayside portion of this current layer, this plasma is accelerated away from the subsolar point by the $\underline{I}\times\underline{B}_n$ force, where $\underline{I}$ is the magnetopause current, to form a boundary layer of jetting plasma immediately inside the magnetopause. Tailward of the two cusp regions, the direction of $\underline{I}$ is reversed so that the plasma is decelerated instead (a feature not included in the Levy et al. model). It is in these latter regions that mechanical energy is extracted from the solar wind and stored as magnetic energy in the geomagnetic tail (e.g., Swift, 1980). However, the presence of such deceleration regions is merely a consequence of ongoing reconnection somewhere on the subsolar magnetopause. For this reason, we shall focus attention on this latter region.

In the Levy et al. model (Fig. 2), it was assumed that no plasma is present in the magnetosphere. As a result, the inner edge of the plasma boundary layer inside the magnetopause consists of a narrow slow-mode expansion

fan in which the plasma expands to zero pressure and is accelerated further (see Yang and Sonnerup, 1977). In reality the dilute but hot magnetospheric plasma has a substantial pressure so that the expansion fan may be absent or even replaced by a slow shock. It is not clear how collision-free slow shocks and expansion fans manifest themselves in the narrow magnetopause-boundary layer region.

The rotational discontinuity is expected to be present at the magnetopause in all but the most unusual circumstances: strictly antiparallel fields and identical or nearly identical plasma and field states on the two sides of the magnetopause in which case the usual symmetric Petschek model containing pairs of slow shocks applies. Even a small increase in density outside the magnetopause over that inside is sufficient to bring the outer slow shocks in that model to their maximum strength (switch-off of the tangential field). After that, an RD will appear. If the reconnecting magnetic fields are not antiparallel, an RD is always needed. For these reasons, the principal magnetic and plasma signatures of the magnetopause region away from the separator (reconnection line; X line) should be those associated with an RD.

The separator is usually assumed to pass through the subsolar point on the magnetopause and to be oriented along the net magnetopause current, $\underline{I}$, as illustrated in Fig. 3a. Figure 3b shows that this orientation does not permit reconnection between fields B_1 and B_2, where $B_1<B_2$, for an angle $\Delta\theta$ such that $\cos\Delta\theta\geq B_1/B_2$, because the magnetic field component perpendicular to the separator must reverse sign for reconnection to be possible (see e.g., Sonnerup, 1974). However, Cowley (1976) has argued that the separator orientation along $\underline{I}$, while consistent with theory, may not be required by it. A hypothesis has also been advanced (Crooker, 1979) to the effect that reconnection occurs only at those locations on the magnetopause where B_1 and B_2 are

antiparallel or nearly antiparallel (see J. Luhmann, this Volume). The merits of this suggestion have yet to be evaluated.

Direct observational proof of the occurrence of reconnection would consist of a measured electric field along a separator since that is a standard definition of reconnection. However, this is difficult to accomplish, not only because electric-field measurements in the magnetopause plasma environment are difficult, but also because the diffusion region, i.e., the narrow channel around the separator in which the frozen magnetic field condition is violated, has small physical dimensions and therefore is difficult to identify. The difficulty is compounded by the fact that our theoretical understanding of the important plasma processes in the diffusion region is poor (J.F. Drake, this Volume). In effect, we do not know what plasma signatures to look for. A suggestion concerning a magnetic signature produced by Hall currents may be found in Sonnerup (1979).

It is possible to obtain persuasive evidence for reconnection even from satellite traversals of the magnetopause away from the reconnection site itself, i.e., away from the separator. An electric field E_t tangential to the magnetopause or a magnetic field component B_n normal to it, if present over a region of linear dimensions much greater than the magnetopause thickness, indicates that reconnection is occurring or has occurred in the recent past. According to simple steady-state 2D reconnection theory E_t is equal to the reconnection rate and B_n is proportional to E_t. Both E_t and B_n are difficult to determine: over most parts of the magnetopause, the largest electric field component is normal to the magnetopause (see T. Aggson, this Volume) and the largest magnetic field component is tangential to it. Thus a reliable determination of E_t or B_n depends critically upon the knowledge of a reliable normal vector. Because of wave motion and other irregularities

in the magnetopause surface, a model normal is not useful for this purpose. The remaining possibility is to obtain a normal vector (and B_n) from minimum-variance analysis of the magnetic field data (Sonnerup and Cahill, 1967). Occasionally, reliable normal vectors and B_n values are obtained from this process and there is little doubt (e.g., Sonnerup and Ledley, 1979) that a few magnetopause crossings have been identified where B_n was significantly different from zero. But more often than not, the minimum variance method fails to give a reliable normal vector (and B_n) and so the opportunity to measure the reconnection rate for a given magnetopause crossing is limited. A third quantity which is also proportional to the reconnection rate is the flow velocity component, v_n, across the magnetopause. However, it is difficult to measure and suffers from the same drawback as E_t and B_n, namely, an accurate $\underline{n}$ vector is needed. In addition, a normal flow velocity component is in itself not convincing evidence of reconnection since it could be the result of rapid diffusion of plasma across a TD.

A simple check on the presence or absence of reconnection can be obtained by examination of the behavior of the tangential plasma velocity across the magnetopause. According to the reconnection model, the interplanetary plasma experiences a change in tangential momentum caused by the $\underline{I}\times\underline{B}_n$ force as it crosses the current layer. On the dayside, and with the interplanetary magnetic field due essentially south, the net effect is plasma acceleration to velocities of about twice the Alfvén speed, $2v_A$, leading to the plasma jets shown in Fig. 2, just inside the magnetopause. These jets have indeed been observed (Paschmann et al., 1979, Sonnerup et al., 1981, Gosling et al., 1982), and the observed detailed agreement with the theoretical tangential momentum change makes it unlikely that these jets were the product of processes other than reconnection.

In spite of the fact that the $\underline{I}\times\underline{B}_n$ force is proportional to the reconnection rate via B_n, the plasma momentum change is independent of that rate. The reason is that the mass flow rate, ρv_n, across the magnetopause is also proportional to the reconnection rate. Thus, observations of this type cannot be used to establish the reconnection rate.

There are a number of other direct consequences of the reconnection field topology which are observable in the region between the inner and outer separatrix surfaces, shown in Fig. 2. These surfaces intersect in the diffusion region and they might therefore bear the signature, in the form of heat flow, of any electron heating in that region (see J.D. Scudder, this Volume). In addition, the outer separatrix might be traced by escaping magnetospheric electrons.

Between the outer separatrix and the magnetopause one might expect to find magnetospheric and ionospheric ions that have leaked across the magnetopause and have been given a tangential velocity change of up to $2v_A$ by the $\underline{I}\times\underline{B}_n$ force (Scholer et al., 1981; Sonnerup et al., 1981), as well as magnetosheath ions that have been reflected in the magnetopause and have been similarly influenced by the $I\times B_n$ force (Sonnerup et al., 1981). Between the magnetopause and the inner separatrix, one expects to find, not only the jetting plasma boundary layer, but also any magnetospheric ions that have not leaked across the magnetopause but have been reflected against it (Scholer and Ipavich, 1983). Detailed consideration of these various signatures may be found in G. Paschmann's article (this Volume). Finally, it is noted that the inner separatrix comprises the last set of closed field lines in the magnetosphere. This surface and the region just outside it project into the high-latitude the ionosphere so that many of the consequences of magnetopause reconnection should be observable there (see P. Reiff, this Volume).

3. ROTATIONAL DISCONTINUITY

The basic properties of an RD are: (i) it has a nonvanishing magnetic field component, B_n, normal to the layer; (ii) the plasma flows towards and away from the discontinuity with normal speed, v_n, equal to the Alfvén speed based on B_n and corrected for nonisotropic pressure; (iii) the tangential magnetic field can change direction by an arbitrary angle $\Delta\theta$ across the sheet; indeed, it is the only discontinuity having this capability. The fact that the flow speeds into and out of the discontinuity are equal to the corresponding Alfvén-wave speeds guarantees that no wave steepening or broadening of the usual type is present in a uniform medium.

Jump Conditions

In a collision-free plasma with nonisotropic pressure the jump conditions across an RD are (Hudson, 1970; 1971; 1973):

$$\Delta\{\rho(1-\alpha)\} = 0 \qquad \text{(Mass Cons.)} \qquad (1)$$

$$\Delta\{P_\perp + B^2/2\mu_0\} = 0 \qquad \text{(Normal Mom. Cons.)} \qquad (2)$$

$$\Delta\{\underline{v}_t - \underline{v}_{At}\} = 0 \qquad \text{(Tang. Mom. Cons.)} \qquad (3)$$

$$\Delta\{(\alpha+\tfrac{1}{2})B^2/\mu_0\rho + 5P_\perp/2\rho\} = -q \qquad \text{(Energy Cons.)} \qquad (4)$$

In these equations, the symbols, ρ, p, $\underline{B}$, and $\underline{v}$ have their usual meaning and the delta bracket is defined by $\Delta\{K\} \equiv K_2 - K_1$, where the subscripts 1 and 2 denote conditions upstream and downstream of the discontinuity. Also, q is the amount of energy per unit mass which leaves the system via heat conduction or radiation. The pressure anisotropy, α, is defined by

$$\alpha \equiv (p_\parallel - p_\perp)\mu_0/B^2 \qquad (5)$$

Finally, $\underline{v}_{At} \equiv B_t[(1-\alpha)/\mu_o\rho]^{\frac{1}{2}}$ is the tangential Alfvén speed. In the frame of the RD, the normal plasma flow speeds towards and away from the layer are $v_{x1} = v_{Ax1} = B_x[(1-\alpha_1)/\mu_o\rho_1]^{\frac{1}{2}}$ and $v_{x2} = v_{Ax2}$, respectively. In the fire-hose limit, $\alpha_1 = \alpha_2 = 1$, the plasma ceases to flow across the discontinuity.

From the above formulas with $q=0$ and $\alpha_1=\alpha_2=0$, the well known MHD results (e.g., Landau and Lifshitz, 1960) are recovered: ρ, p, and B remain unchanged across the RD while the direction of $\underline{B}_t$ can change by an arbitrary angle, this change being accompanied by a corresponding change in $\underline{v}_t$ as indicated by Eq. (3). If the tangential field $\underline{B}_t$ rotates by an angle $\Delta\theta$, Eq. (3) yields $|\Delta\underline{v}_t| = 2|\underline{v}_{At}|\sin(\Delta\theta/2)$ so that the maximum value of $|\Delta\underline{v}_t|$ is $2v_{At}$, a result already quoted in Section 2.

If $q=0$ and $\alpha_1=\alpha_2\neq 3/4$, ρ, p, and B again remain constant but the Alfvén speed now contains the correction factor $(1-\alpha)^{\frac{1}{2}}$. This situation arises if the double adiabatic relations $p_\perp/\rho B$ = const. and $p_\parallel B^2/\rho^3$ = const. hold. If only the first of these conditions, representing the conservation of the magnetic moment of a particle, is valid, a curious situation arises (Hudson, 1973). One possible root is $\alpha_2=\alpha_1$ in which case ρ, p, and B all remain unchanged. But there also exist parameter ranges in which a second root $\alpha_2\neq\alpha_1$ occurs in which case ρ, p, and B all change across the RD. In discontinuities of this type the entropy usually also changes: for $q=0$ only solutions that bring about an entropy increase, $\Delta\{s\}>0$, are physically acceptable. If neither of the adiabatic relations hold and/or if $q\neq 0$, even more general behavior appears possible.

In summary, contrary to the case of shocks, the jump conditions across a rotational discontinuity do not uniquely specify the change of state of the plasma and field. As long as $q=0$, one possibility is always that the plasma state and field magnitude remain unchanged but other possibilities

exist as well. These have been explored to some extent by Hudson (1971, 1973). However, recent experimental evidence (G. Paschmann, this Volume) indicates that substantial ion heat flow away from the magnetopause RD occurs occasionally so that the assumption q=0 is not always a good one.

Structure

The structure and thickness of the rotational discontinuity must be such that the changes implied by the jump conditions are achieved. For example, one must presume that the two conditions q=0 and $\Delta\{s\}=0$ together imply a sufficient thickness of the layer so as to permit laminar, non-dissipative behavior of the plasma. It also seems likely that limitations derived from the RD structure may eliminate certain downstream states that are allowed by the jump conditions.

In dissipationless MHD, the RD structure is simple: the plasma state and the magnetic field magnitude remain constant while the angle, θ, of the tangential field changes by the desired amount, $\Delta\theta$. The function $\theta(x)$, x being the normal coordinate, can be specified arbitrarily. If a small amount of dissipation is present, the width of the layer increases gradually.

Our theoretical knowledge of the structure of rotational discontinuities in a collision-free plasma is not extensive and is limited to laminar structures, as discussed below. However, observations (e.g., Sonnerup and Ledley, 1979; Berchem and Russell, 1982; Paschmann et al., 1979) suggest that in reality the structure may be turbulent.

In analyzing the structure of current layers, it is convenient to use the so-called de Hoffmann-Teller (dHT) frame in which the external electric field vanishes (such a frame can be found for all plane one-dimensional layers except perpendicular shocks). In this frame, the inflow and outflow velocities at an RD are field aligned and equal to the Alfvén speeds on the two sides.

The following basic statements can be made:

(1) The structure of a rotational discontinuity involves an electric field $E_n(x)$ normal to the layer and an associated potential barrier $\phi(x)$. The first-order orbit theory model examined by Su and Sonnerup (1968) as well as the double-adiabatic model by Lee and Kan (1982) contains such an electric field. But it can be shown in a general way (Sonnerup and Wang, 1984) that, regardless of model, an RD must always contain a potential barrier. Su and Sonnerup recognized the possibility of trapping particles electrostatically in the layer but they did not satisfy charge neutrality (or Poisson's equation). Lee and Kan were the first to understand the crucial role played by trapped electrons in this regard and theirs is the only complete model in print to date. It predicts E_n values of the order of one millivolt per meter for typical magnetopause conditions. However, recently Wang and Sonnerup (1983a,b) have developed a model in which large deviations from charge neutrality occur in narrow regions (electrostatic "shocks") of width equal to a few Debye lengths. The electric fields in these narrow regions are of the order of volts per meter.

It should be noted that both $E_n(x)$ and $\theta(x)$ change when one transforms from the dHT frame to some other frame of reference (the lab frame) moving parallel to the discontinuity. This must be kept in mind when comparing electric field measurements to theory.

(2) For an RD in a plasma consisting of electrons with isotropic pressure tensor and one specie of ions of charge q, the tangential magnetic field, $B_t=B_y+iB_z$, where $i^2=-1$, can be shown to obey the equation (Sonnerup and Wang, 1984)

$$\frac{dB_t}{dx} = iB_t \frac{\sqrt{1-\alpha_1}}{\lambda_{i1}} \left[1 - \frac{n_i}{n_{i1}} \left(1 - \frac{\mu_o P_{ixt}}{B_x B_t} \right) / (1-\alpha_1) \right] \qquad (6)$$

where $\lambda_{i1} \equiv (m_i/\mu_o n_{i1} q^2)^{\frac{1}{2}}$ is the ion inertial length, n_{i1} is the ion number density, and α_1 is the pressure anisotropy factor, upstream of the RD. Also $P_{ixt} \equiv P_{ixy}+iP_{ixz}$ is the tangential ion stress. Note that because $n_{i1}(1-\alpha_1) = n_{i2}(1-\alpha_2)$ all upstream conditions (subscript 1) can be replaced by downstream ones (subscript 2). It is easy to show that for the upstream or downstream state, $P_{ixt} = B_x B_t \alpha/\mu_o$ so that $dB_t/dx = 0$ there.

In the absence of viscous stresses, the ion pressure tensor P_i is diagonal in a coordinate system with one axis along $\underline{B}$. In that case P_{ixt} is proportional to B_t so that the ratio P_{ixt}/B_t is purely real. Equation (6) is then of the form $dB_t/dx = ig(x)B_t$, where $g(x)$ is a real function of x, indicating that the field magnitude $|B_t|$ is constant.

In magnetopause rotational discontinuities the magnetic field magnitude often has a minimum in the center of the layer. The above results indicate that such an effect is likely to be caused by viscous stresses in the layer (although nonisotropy of the electron stress tensor and/or the presence of more than one ion specie may be contributing factors as well). Viscous stresses are expected to be important only in thin layers so that strong deviations from $|B_t|$=const. should be an indication that the magnetopause width is small.

(3) Equation (6) also forms a suitable basis for discussing the sense of polarization of the RD. The right-hand (electron) and left-hand (ion) polarizations are obtained when the rectangular bracket is positive and negative, respectively. For example, if the ions are cold so that P_{ixt}=0, α_1=0, then the ion polarization is obtained for a positive potential barrier, $\phi(x)>0$, since such a barrier will lead to $n_i > n_{i1}$. Similarly, $\phi(x)<0$ yields the electron polarization. For hot ions, the situation is less well understood. For example, in the double-adiabatic description of the ions employed

by Lee and Kan (1982) the square bracket reduces to $[1-n_i/n_{i1}]$ but for $\phi(x)>0$ (the only case dealt with by Lee and Kan) the density ratio n_i/n_{i1} is found to be less than unity except for cold or almost cold ions, the result being the electron polarization.

Sonnerup and Ledley (1979) have argued that only the electron polarization should occur for layers that are sufficiently thin so that only electrons but not ions are capable of moving across the layer by sliding along the magnetic field lines so as to provide the required field-aligned current distribution in the layer. This situation should arise when the layer thickness is comparable to, or less than, the ion gyroradius. On the basis of Explorer 12 and OGO5 data, these authors also state that both polarizations have been observed but with a preference for the electron sense. On the other hand, Berchem and Russell (1982) (see also Russell, this Volume) have found from ISEE data that the basic polarization rule is for the field rotation angle $\Delta\theta$ in the layer to obey the inequality $\Delta\theta<\pi$. However, these authors did not distinguish between rotational and tangential discontinuities so that the distribution among the former between the ion and electron polarization in their data set remains unknown. However, examination of published Explorer 12 and OGO5 RD's basically supports the Berchem and Russell rule. Only one crossing has been published in which $\Delta\theta>\pi$ (Sonnerup and Ledley, 1974). This crossing had the electron polarization.

Further support for the rule $\Delta\theta<\pi$ comes from a recent computer simulation of RD's by Swift and Lee (1983) in which cases with $\Delta\theta>\pi$ were observed to be unstable. The reason for this effect is not clear.

4. PARTICLE ORBITS

Motion in de Hoffmann-Teller Frame

In this section we review certain general results concerning particle orbits in one-dimensional current sheets with $B_x = B_n \neq 0$. It is advantageous to study the orbits in the dHT frame because in that frame particles have simple helical orbits as they travel towards and away from the current sheet. In the sheet itself their motion may be extremely complicated but it remains constrained by the conservation of total energy and the two generalized tangential momenta:

$$mv^2/2 + q\phi(x) = \text{const.} \tag{7}$$

$$mv_y - qB_x z + qA_y(x) = \text{const.} \tag{8}$$

$$mv_z + qB_x y + qA_z(x) = \text{const.} \tag{9}$$

where $B_y \equiv -dA_z/dx$ and $B_z \equiv dA_y/dx$ are the field components tangential to the layer.

Cowley (1978) has shown that Eqs. (7), (8), and (9) constrain the particle orbit to lie inside a surface in space, the intersection of which with any plane parallel to the yz plane is circular with radius $R_x = mv/qB_x$. As one moves from one plane parallel to the yz plane to another, R_x changes as the particle speed v changes in response to $\phi(x)$. The center of the circle moves in such a way that it remains located on one and the same field line.

It is instructive to arrive at these results by use of the diagrams in Fig. 4. As shown in part (a) of that figure, at a given fixed x value, the position of a particle in velocity space is constrained to lie on a sphere of radius v where $v = v_1\sqrt{1-2q\phi(x)/m}$, v_1 being the particle speed upstream of

the current layer where ϕ=0. On this sphere the circles which represent constant pitch angles, α, with respect to the local magnetic field are shown for convenience. If the geometry shown in Fig. 4a is projected onto the v_y v_z plane, the result is the circular disk $v_y^2 + v_z^2 \leq v^2$ shown in Fig. 4b. The circles of constant pitch angle now appear as ellipses inside the disk. The cases α=0, corresponding to particle motion along $\underline{B}$ towards increasing x, and $\alpha=\pi$, corresponding to motion along $\underline{B}$ towards decreasing x, appear as two points labeled, 0 and π, respectively. For a fixed x value, Eqs. (8) and (9) provide a linear transformation from the tangential velocity map in Fig. 4b to a plane in configuration space parallel to the yz plane and located at the assumed x value. This transformation consists of a clockwise rotation of the disk and a scaling by the factor m/qB_x, as shown in Fig. 4c.

The terms $A_y(x)$ and $A_z(x)$ in the transformation lead to a shift of the disk location with changing x value such that the center remains on one and the same field line. To see this, we differentiate Eqs. (8) and (9) to obtain

$$B_x dz = (dA_y/dx)dx = B_z dx \tag{10}$$

$$B_x dy = (-dA_z/dx)dx = B_y dx \tag{11}$$

which are the differential equations for a field line.

In the uniform field region on either side of the current layer, the surface traced by the disk (Fig. 4d) is a cylinder of elliptical cross section as shown in Fig. 4e for the upstream side, say, of the layer. In the figure, the symbol φ denotes the angle between the incident magnetic field, assumed to lie in the xy plane, and the surface of the discontinuity. Inside the ellipse are circles with centers at $z = (mv/qB_x)\cos\varphi\cos\alpha$, each labeled by a corresponding pitch angle, α. For $0 \leq \alpha < \pi/2$ the particle moves

in a helical orbit toward the layer while for $\pi/2<\alpha\leq\pi$ it moves away from it. The two foci of the ellipse correspond to $\alpha=0$ and $\alpha=\pi$. For pitch angles near 0 and π, the circles do not touch the ellipse: they correspond to helices in which v_x does not change sign. For circles that touch the ellipse, v_x changes sign at the points of osculation.

As a simple illustration of Fig. 4e, consider a particle incident upon the current sheet with pitch angle α_1 ($<\pi/2$) which is reflected and leaves with pitch angle α_2 ($>\pi/2$). Figure 4e shows that during the interaction with the current sheet, the guiding center of the particle is displaced by the distance

$$\Delta z = \frac{mv}{qB_x}\cos\varphi\,(\cos\alpha_1-\cos\alpha_2) \qquad (12)$$

i.e., purely in the z direction. The maximum displacement occurs when $\alpha_1=0$, $\alpha_2=\pi$, in which case the orbit moves from one focus of the ellipse to the other (a result that may be compared to the approximation used by T.W. Speiser, this Volume).

A second illustration is provided in Fig. 5 which shows a view along the normal, i.e., along the positive x direction of a rotational discontinuity with $\Delta\theta=135^\circ$. A field line bends, as shown in the figure, as it passes through the current layer. Disks are shown at the entrance to (#1), in the middle of (#1½), and at the exit from (#2) the layer. Note that the constant pitch angle pattern in the disk rotates as one progresses through the current layer. Disks #1 and #2 are shown with the same diameter, corresponding to an assumed value $\phi=0$ of the electric potential on both sides of the layer. Disk #1½ has a smaller diameter corresponding to the assumed presence of a potential barrier $\phi(x)$. As an example, a particle with zero pitch angle enters the layer at the point $\alpha=0$ in disk #1. If the magnetic moment μ is preserved, it leaves at the point $\alpha=0$ in disk #2. Note that

because of inertia drift it does not follow the field line through the entry point which leaves the layer at the point labeled P. If the particle were reflected rather than transmitted it would leave at the point $\alpha=\pi$ in disk #1 instead (assuming constant μ). In reality, the magnetic moment is not necessarily preserved and numerical orbit calculations are needed to obtain the exit pitch angle.

Particle Energization

Equation (3) describes the tangential momentum change of the plasma as it crosses an RD. Depending on circumstances, this change will lead either to energization or to deenergization of the plasma. These effects can be examined by transforming velocities from the dHT frame to the "laboratory" frame. As illustrated in Fig. 6, this transformation consists of adding a constant velocity $\underline{v}_0$ parallel to the sheet. Energization of transmitted and reflected particles is illustrated in Figs. 6b and 6c while an example of deenergization is shown in Fig. 6d. For simplicity, only the case where $\underline{B}_1$, $\underline{B}_2$, and $\underline{v}_0$ all lie in the xy plane is shown.

In the laboratory frame a constant tangential electric field, $\underline{E}_t = -\underline{v}_0 \times \underline{B}_n$, will be present, the direction of which is shown in Fig. 6. This is the reconnection electric field, and it now becomes clear that $\underline{E}_t$ and B_n are indeed proportional. At the magnetopause $\underline{E}_t$ is a remnant of the interplanetary electric field (IEF) and is directed from dawn to dusk for southward interplanetary magnetic field (IMF). Note that $\underline{E}_t \cdot \underline{I} > 0$ for energization and $\underline{E}_t \cdot \underline{I} < 0$ for deenergization. The former case occurs on the frontside magnetopause where the magnetopause current, $\underline{I}$, is directed from dawn to dusk for southward IMF. The latter case occurs on portions of the magnetopause tailward of the cusp where $\underline{I}$ is directed from dusk to dawn. The suggestion has been made (Crooker, 1979) that it may also occur on the

frontside magnetopause as a consequence of cusp reconnection. But since $\underline{I}$ is directed from dawn to dusk on the frontside, $\underline{E}_t$ would then have to be directed from dusk to dawn, i.e., it would have to oppose the IEF. This appears unlikely.

The energization or deenergization of individual particles occurs as a result of a displacement of the particle guiding center along $\underline{E}_t$. As an example, consider a particle reflected at the current layer. It is easy to show from the velocity triangles in Fig. 6c that the kinetic energy increase is

$$\Delta\varepsilon = mvv_0\cos\varphi(\cos\alpha_1-\cos\alpha_2) \equiv qE_t\Delta z \qquad (13)$$

(Note that $\alpha_2>\pi/2$) where Δz is the guiding center displacement. Since $v_0 = E_t/B_n = E_t/B_x$ we can solve this expression for Δz, the result being exactly the displacement given by Eq. (12). In other words, orbit considerations based on the conservation of energy and generalized tangential momenta lead to exactly the same result as the frame transformation method described in Fig. 6. This is not surprising but it serves to emphasize that the MHD reconnection model which predicts plasma acceleration by the $\underline{I}\times\underline{B}_n$ force is internally consistent: the reconnection electric field is precisely the field needed to energize the plasma particles by the requisite amount. Thus experimental checks of the tangential momentum balance automatically provide a check of the electromechanical part of the energy balance. However, the remaining, thermal part is in general not negligible (see G. Paschmann, this Volume).

Equation (12) indicates that the particle displacement Δz along E_t becomes very large as $B_x=B_n$ approaches zero. However, at the same time E_t itself becomes small, the result being that the energy gain $\Delta\varepsilon$ remains the

same. Therefore, as stated earlier the plasma energization is independent of the reconnection rate. It is also evident from Eq. (12) that the energization of electrons is negligible compared to that of the ions.

The general formula for the energization of a particle transmitted through an RD, as illustrated in Fig. 5, is not much more difficult to work out than the simple case of reflected particles discussed above. For example, a particle which crosses the layer while retaining $\alpha=0$ will undergo an effective tangential displacement $\Delta\underline{r}_t$ from point P to point $\alpha=0$ in disk #2 so that its energy increase will be $\Delta\varepsilon = q\underline{E}_t\cdot\Delta\underline{r}_t$. The reason that the distance from the point $\alpha=0$ in disk #1 to the point P is not included in $\Delta\underline{r}_t$ is that these two points have the same electric potential: the total transformation electric field $\underline{E}_0 = -\underline{v}_0\times\underline{B}$ has no component along $\underline{B}$ and the two points are located on one and the same field line. However, as mentioned already in Section 3, $\underline{E}_0$ does have a substantial component along the normal direction.

5. NONSTEADY LOCALIZED RECONNECTION

The preceding sections have dealt with reconnection as a steady-state process. However, there is mounting evidence (Russell and Elphic, 1978; Cowley, 1982) that a nonsteady patchy version of reconnection, referred to as flux transfer events (FTE's), may be the dominant reconnection mode at the magnetopause. The FTE is envisaged as a pair of flux tubes, one in each hemisphere, each passing through a "hole" in the magnetopause and connecting to the earth and each being accelerated along it away from the subsolar region by the magnetic tension associated with the sharp kink in the tube at the hole (see Fig. 7a). Such tubes seem to have typical cross-sectional dimensions of the order of 1 R_E (implying a hole dimension of a few R_E since B_n<B) but in reality there may be a continuum of sizes ranging from dimensions comparable to the ion gyroradius up to the scale of quasisteady reconnection. Detailed discussion of the morphology and statistics of FTE's may be found elsewhere in this Volume. Here a few general remarks are offered concerning these structures and their relation to reconnection.

(1) As illustrated in Fig. 7b, the pair of holes in the magnetopause associated with FTE's must be the result of reconnection, limited to a narrow longitude interval, which started near the equatorial region and then ceased almost immediately before a steady state could be established, the method of cessation being conversion of the reconnection line into two passive or almost passive X lines and an O line.

(2) If quasi-steady reconnection takes place in a limited longitude segment then, for $\Delta\theta \neq \pi$, there are regions on the magnetopause surface where one would observe open field lines but not the plasma jetting discussed previously. Signatures of this type should be looked for in the data and

their relation to FTE's should be examined in detail.

(3) Whenever the IMF is due south, the magnetopause situation would seem to be an ideal one for quasisteady reconnection to occur at its maximum permitted rate. Yet, this is apparently not what happens. Even with a southward IMF, quasisteady reconnection is observed only occasionally, indicating that the process occurs sporadically and/or that it is limited to narrow longitude segments. If the currently popular interpretation of FTE signatures is correct, then what is observed most of the time is therefore a patchy time-dependent version of reconnection. This set of circumstances indicates the existence of a threshold (other than a southward IMF) for the onset of the process. Either by design or by accident the magnetopause plasma state seems to hover around this threshold.

(4) The detailed nature of the threshold is not understood but the following scenario illustrates how FTE's might be generated. Assume that a flux tube containing interplanetary magnetic field lines drapes over the subsolar magnetopause and gets hung up there, perhaps in a preexisting indentation. The plasma in this tube will then escape by flowing tailward along the lines of force, the result being a lowering of plasma density, n, β value (in particular $\beta_{\parallel}$), and Alfvén Mach number, M_A, of the flow. It may be argued that each of these factors is conducive to the onset of reconnection between the field lines in the flux tube and the geomagnetic field. As soon as reconnection has been initiated, two developments occur: (i) a deepening of the indentation in the magnetopause associated with the flux tube must take place as reconnection erodes flux from the magnetosphere; (ii) the region occupied by the original flux tube gets replenished with fresh solar-wind plasma in which n, β, and M_A return to their original values. Via the threshold, the latter effect may lead to the cessation of reconnection.

The former effect creates a suitable trap for new interplanetary magnetic flux tubes. These indentations and reconnection regions may also get swept away over the flanks of the magnetopause so that FTE's should be observable over the entire frontside magnetopause and not just near local noon. And on occasion, the O-type null line created when reconnection ceases (see Fig. 7b) may be swept over one or the other of the poles so that FTE signatures characteristic of the southern hemisphere may occasionally be observed in the northern hemisphere and vice versa.

It also seems reasonable to assume that for suitable plasma conditions a quasisteady reconnection configuration may be established which either remains limited to a narrow longitude segment or spreads over a substantial part of the frontside magnetopause.

The above scenario is by no means unique, but it may serve as a useful guide for future theoretical and observational studies of FTE's. In particular, it illustrates the importance of developing a better understanding of the threshold conditions for onset of magnetopause reconnection. It seems clear that these thresholds must be associated with local conditions at the reconnection site rather than with global boundary conditions. A complete theory is needed for the onset and evolution of the tearing mode in a collision-free plasma when the magnetic field exhibits strong shear as it usually does in the magnetopause current layer.

ACKNOWLEDGEMENT

The research was supported by the Division of Atmospheric Sciences, National Science Foundation, under Grant ATM-8201974, and by the National Aeronautics and Space Administration by Grant NSG5348 to Dartmouth College.

REFERENCES

Berchem, J. and C.T. Russell, Magnetic field rotation through the magnetopause, J. Geophys. Res., 87, 8139, 1982.

Cowley, S.W.H., Comments on the merging of nonantiparallel fields, J. Geophys. Res., 81, 3455, 1976.

Cowley, S.W.H., A note on the motion of charged particles in one-dimensional magnetic current sheets, Planet. Space Sci., 26, 539, 1978.

Cowley, S.W.H., The causes of convection in the earth's magnetosphere: a review of developments during the IMS, Revs. Geophys. Space Phys., 20, 531, 1982.

Crooker, N.U., Dayside merging and cusp geometry, J. Geophys. Res., 84, 951, 1979.

Dungey, J.W., Interplanetary magnetic field and the auroral zones, Phys. Rev. Lett., 6, 47, 1961.

Gosling, J.T., J.R. Asbridge, S.J. Bame, W.C. Feldman, G. Paschmann, N. Sckopke, and C.T. Russell, Evidence for quasi-stationary reconnection at the day-side magnetopause, J. Geophys. Res., 87, 2147, 1982.

Hudson, P.D., Discontinuities in an anisotropic plasma and their identification in the solar wind, Planet. Space Sci., 18, 1611, 1970.

Hudson, P.D., Rotational discontinuities in an anisotropic plasma, Planet. Space Sci., 19, 1693, 1971.

Hudson, P.D., Rotational discontinuities in an anisotropic plasma - II, Planet. Space Sci., 21, 475, 1973.

Johnson, F.S., The gross character of the geomagnetic field in the solar wind, J. Geophys. Res., 65, 3049, 1960.

Landau, L.D. and E.M. Lifshitz, Electrodynamics of Continuous Media, p. 224 Pergamon Press, New York, 1960.

Lee, L.C. and J.R. Kan, Structure of the magnetopause rotational discontinuity, J. Geophys. Res., 87, 139, 1982.

Levy, R.H., H.E. Petschek, and G.L. Siscoe, Aerodynamic aspects of the magnetospheric flow, AIAA J., 2, 2065, 1964.

Paschmann, G., B.U.Ö. Sonnerup, I. Papamastorakis, N. Sckopke, G. Haerendel, S.J. Bame, J.R. Asbridge, J.T. Gosling, C.T. Russell and R.C. Elphic, Plasma acceleration at the earth's magnetopause: evidence for reconnection, Nature, 282, 243, 1979.

Russell, C.T. and R.C. Elphic, Initial ISEE magnetometer results: magnetopause observations, Space Sci. Rev., 22, 681, 1978.

Scholer, M., F.M. Ipavich, G. Gloeckler, D. Hovestadt, and B. Klecker, Leakage of magnetospheric ions into the magnetosheath along reconnected field lines at the dayside magnetopause, J. Geophys. Res., 86, 1299, 1981.

Scholer, M. and F.M. Ipavich, Interaction of ring current ions with the magnetopause, J. Geophys. Res., 88, 6937, 1983.

Sonnerup, B.U.Ö., Magnetopause reconnection rate, J. Geophys. Res., 79, 1546, 1974.

Sonnerup, B.U.Ö., Magnetic field reconnection, in Solar System Plasma Physics (L.J. Lanzerotti, C.F. Kennel, and E.N. Parker, eds.), p. 45, North Holland, Amsterdam, 1979.

Sonnerup, B.U.Ö. and L.J. Cahill, Jr., Magnetopause structure and attitude from Explorer 12 observations, J. Geophys. Res., 72, 171, 1967.

Sonnerup, B.U.Ö. and B.G. Ledley, Magnetopause rotational forms, J. Geophys. Res., 79, 4309, 1974.

Sonnerup, B.U.Ö. and B.G. Ledley, Electromagnetic structure of the magnetopause and boundary layer, in Magnetospheric Boundary Layers (B. Battrick, ed.), p. 401, ESA Scientific and Technical Publ. Branch, Noordwijk, 1979.

Sonnerup, B.U.Ö., G. Paschmann, I. Papamastorakis, N. Sckopke, G. Haerendel, S.J. Bame, J.R. Asbridge, J.T. Gosling and C.T. Russell, Evidence for magnetic field reconnection at the earth's magnetopause, J. Geophys. Res., 86, 10049, 1981.

Sonnerup, B.U.Ö. and D.-J. Wang, Theorems concerning the rotational discontinuity, to be submitted to J. Geophys. Res., 1984.

Su, S.-Y. and B.U.Ö. Sonnerup, First-order orbit theory of the rotational discontinuity, Phys. Fluids, 11, 851, 1968.

Swift, D.W., Substorms and magnetospheric energy transfer processes, in Dynamics of the Magnetosphere (S.-I. Akasofu, ed.), p. 327, D. Reidel Publ. Co., Dorcrecht, 1980.

Swift, D.W. and L.C. Lee, Rotational discontinuities and the structure of the magnetopause, J. Geophys. Res., 88, 111, 1983.

Wang, D.-J., and B.U.Ö. Sonnerup, Electrostatic structure of the rotational discontinuity: the elementary pulse, submitted to Phys. Fluids, 1983a.

Wang, D.-J., and B.U.Ö. Sonnerup, Electrostatic structure of the rotational discontinuity: trapped particles, to be submitted to Phys. Fluids, 1983b.

Yang, C.-K., and B.U.Ö. Sonnerup, Compressible magnetopause reconnection, J. Geophys. Res., 82, 699, 1977.

FIGURE CAPTIONS

Fig. 1 The first reconnection model of the magnetosphere (Dungey, 1961). The reconnection electric field E_t, which leads to the flow pattern shown, is comparable in size to the interplanetary electric field so that most of the incident magnetic flux becomes interconnected with the earth's field.

Fig. 2 Magnetopause reconnection model due to Levy et al. (1964) in which only a small portion of the incident magnetic flux is reconnected. The principal geometrical features of this model are: the separator (X); the magnetopause current layer in the form of a rotational discontinuity (RD); a thin high-velocity plasma boundary layer (BL) immediately inside the magnetopause and, at its innermost edge, a slow-mode expansion fan (SEF; shown shaded). The inner and outer separatrix surfaces are marked by (IS) and (OS), the reconnection electric field by E_t, and the magnetopause current by I.

Fig. 3 (a) The separator (X line) is aligned with the net magnetopause current I. (b) For $\cos\Delta\theta > B_1/B_2$ no reconnection is possible.

Fig. 4 (a) In the de Hoffmann-Teller frame, and at a fixed x value, a particle is located on a sphere of radius v in velocity space. Circles of constant pitch angle on this sphere are shown. (b) Projection of the sphere and the constant-pitch-angle circles on the $v_y v_z$ plane. (c) The generalized tangential momenta provide a linear transformation from the $v_y v_z$ plane to the yz plane. (d) Surface in space traced by the disk (c) as x is changed. (e) Elliptic cross section of the surface (d) on left-hand side of current layer.

Fig. 5 View of the magnetopause from the sun. The interplanetary field B_1 connects with the magnetospheric field B_2 across the magnetopause. Cowley's (1978) disks are shown outside (#1), in the middle of (#1½), and inside (#2) the magnetopause.

Fig. 6 Velocity change of a particle as it interacts with the magnetopause current layer (shaded). (a) In the de Hoffmann-Teller frame, a transmitted particle has velocities $v_1 = v\cos\alpha_1$ and $v_2 = v\cos\alpha_2$ before and after the interaction. (b) In the laboratory frame a transformation velocity $\underline{v}_0$ has been added and the particle now has velocities v_1' and v_2' instead where $v_2' >> v_1'$. (c) A reflected particle is similarly energized. (d) De-energization is achieved by reversing the direction of $\underline{v}_0$. The magnetopause current $\underline{I}$ and the electric field $\underline{E}_t = -\underline{v}_0 \times \underline{B}_n$ are parallel for energization, antiparallel for de-energization.

Fig. 7 (a) View from the sun of a flux transfer event (FTE) on the magnetopause. (b) Side view of the magnetopause (shaded) during the development of an FTE. At t=0 the frontside magnetopause is closed, with an O-type magnetic null line at the subsolar point. Reconnection starts, splitting the O-line into two O-lines and an X line, the latter remaining at the subsolar point. At t=1 all the magnetic flux comprising the original magnetopause has been reconnected. At t=2 some interplanetary magnetic field, B_1, has become connected to the earth's field, B_2. At this time, the X line is converted to an O-line and two X lines, the former remaining at the subsolar point. A small amount of reconnection occurs at the two X lines, the result being the formation of a closed magnetopause near the subsolar point at t=3, along with two separate holes in the magnetopause. The situation at t=3 corresponds to the section A-A in part (a) of the figure.

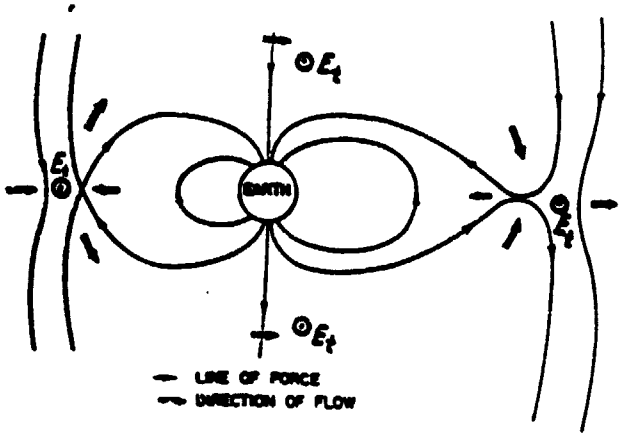

Fig. 1.

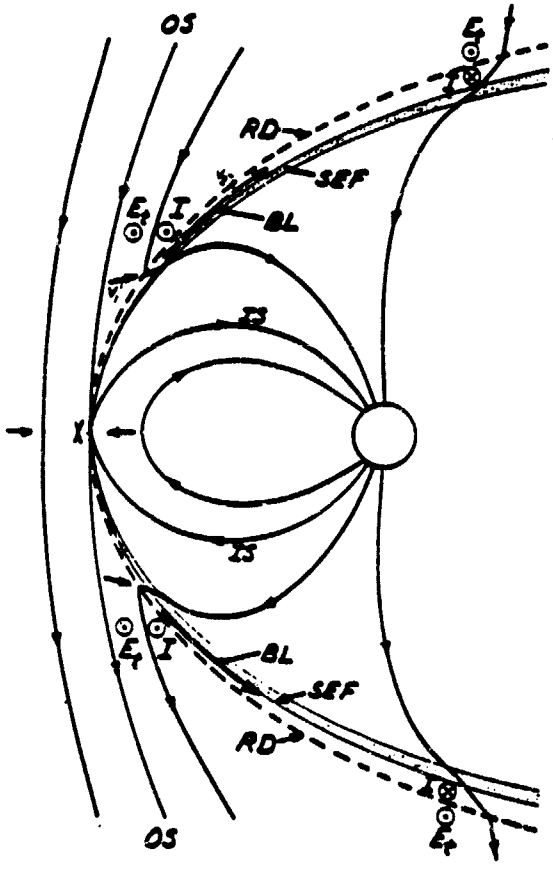

Fig. 2

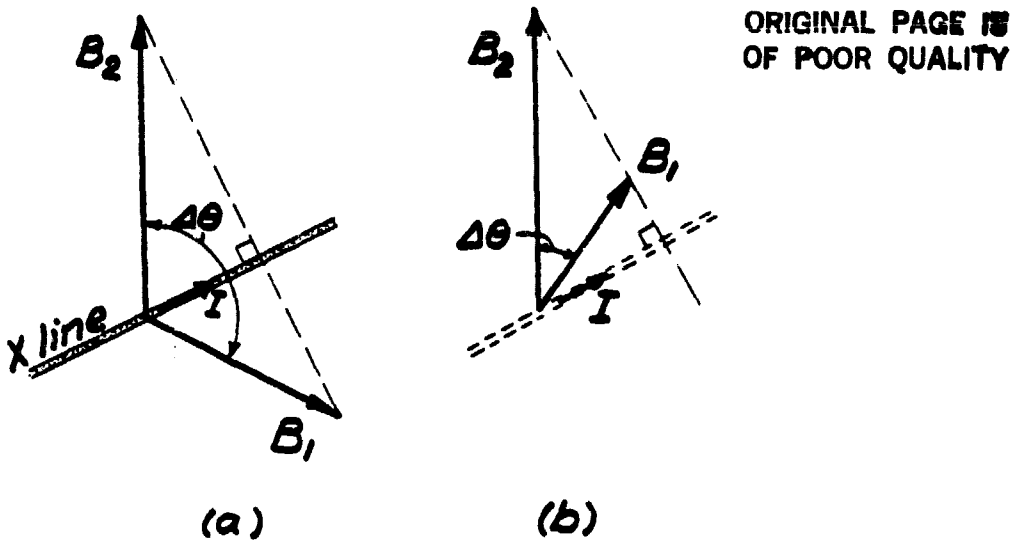

Fig. 3

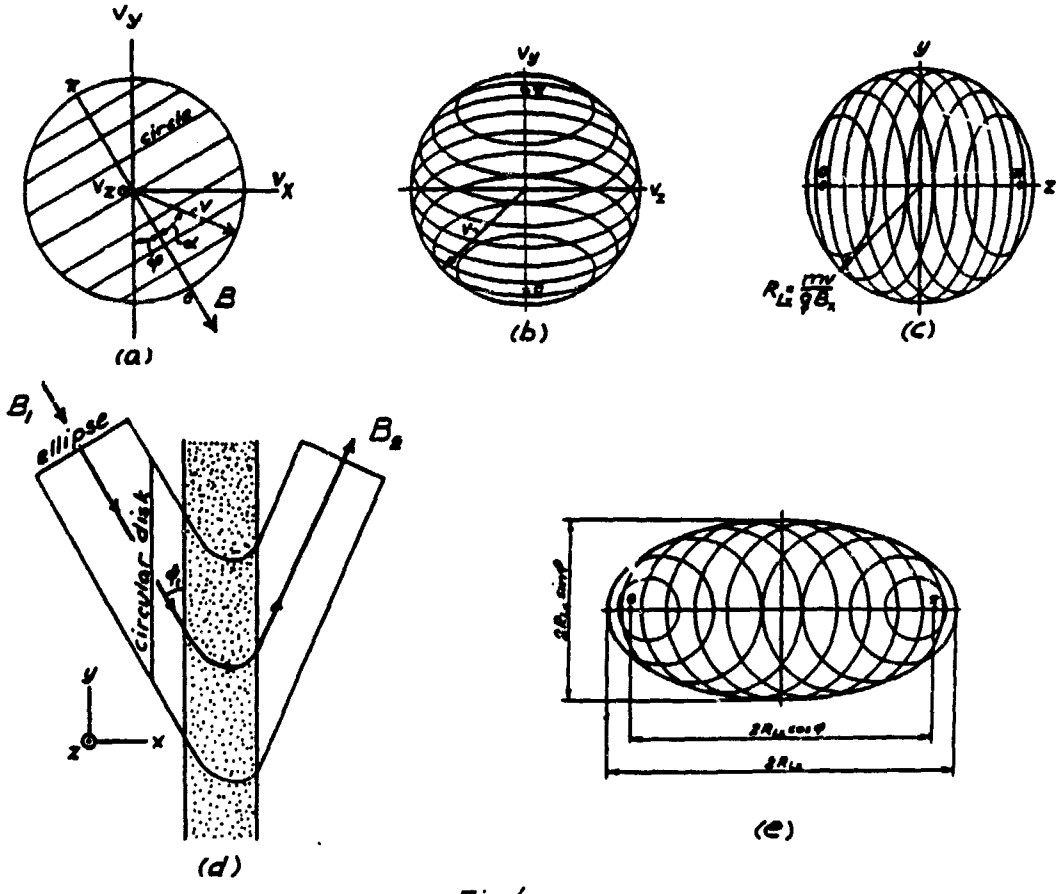

Fig. 4

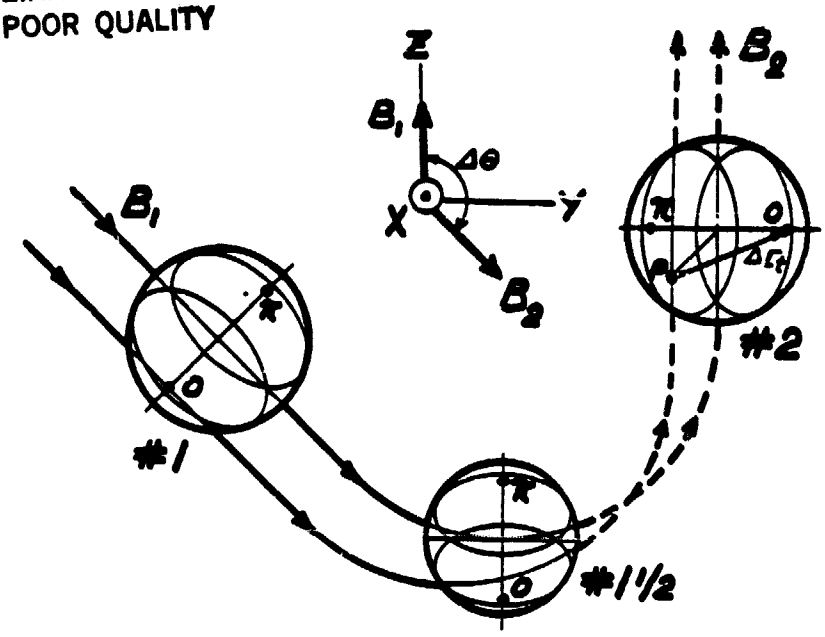

Fig. 5

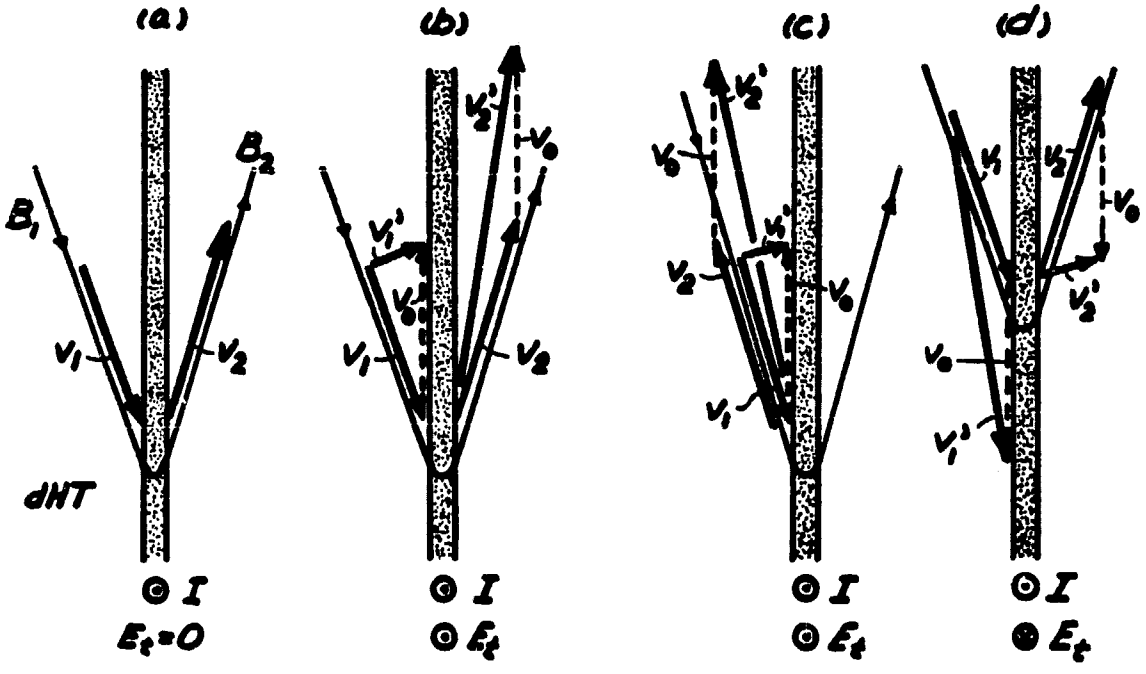

Fig. 6

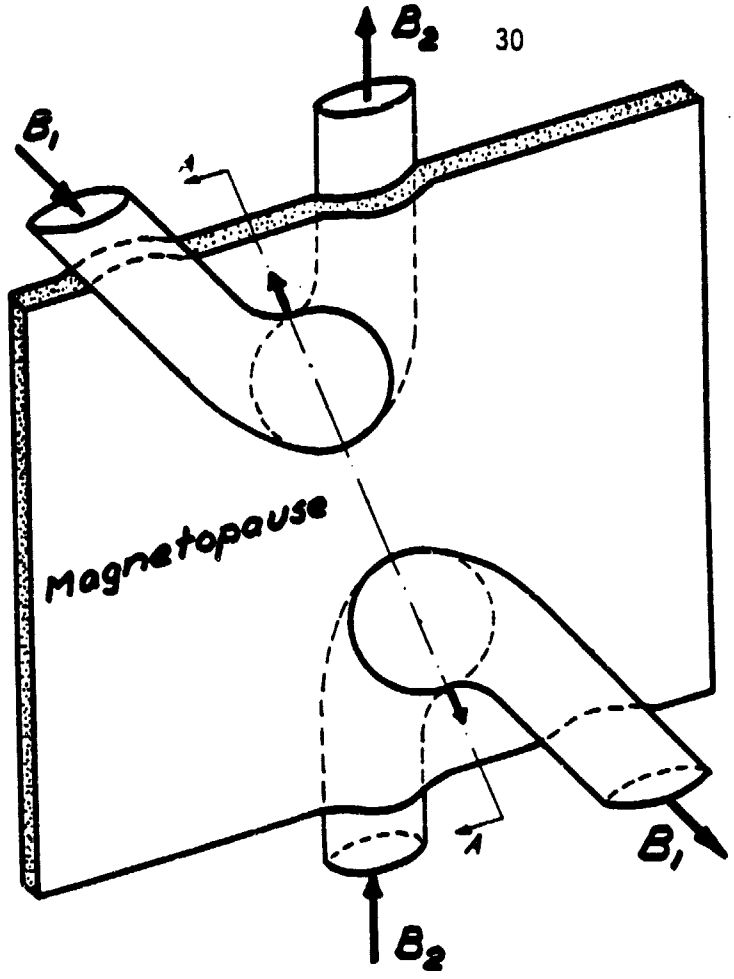

(a)

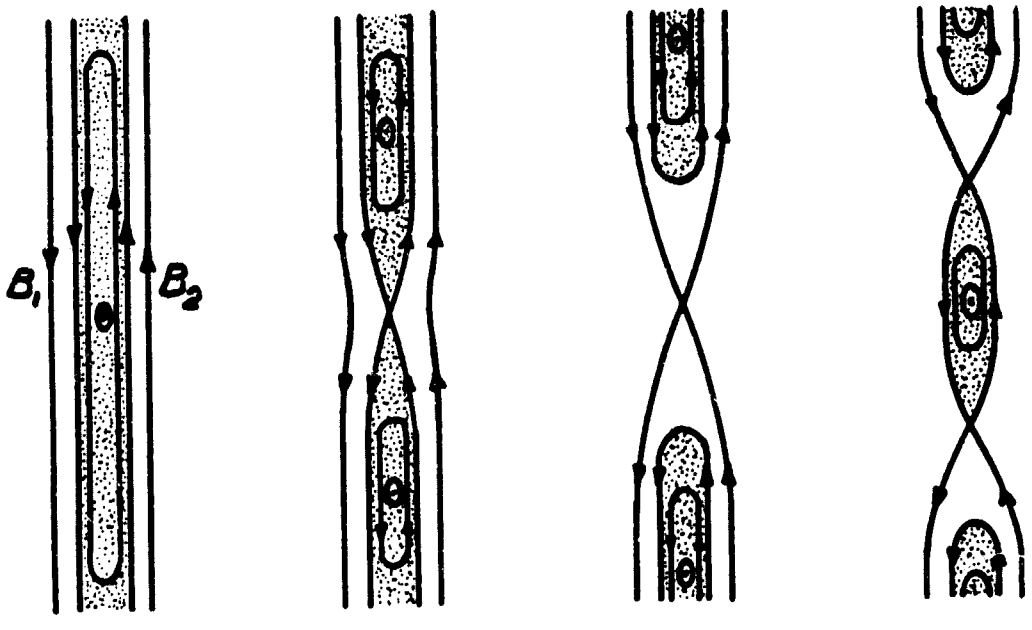

(b)

Fig. 7

DRAFT

D2

N84 17720

ISEE OBSERVATIONS OF MAGNETOPAUSE RECONNECTION: THE ENERGY BALANCE

G. Paschmann, I. Papamastorakis, N. Sckopke,
Max Planck Inst. for Extraterr. Physics, 8046 Garching, FRG.
B.U.Ö. Sonnerup,
Dartmouth College, Hanover, NH 03755.
S.J. Bame,
Los Alamos National Laboratory, Los Alamos, NM 87545.
C.T. Russell,
University of California, Los Angeles, CA 90024.

ABSTRACT

According to the usual magnetopause reconnection model, plasma flows across the magnetopause current sheet, which is a rotational discontinuity with a nonzero normal magnetic field component B_n, from the magnetosheath into the magnetospheric boundary layer. As the plasma crosses the sheet, which has net current I, it is accelerated by the $\underline{I}\times\underline{B}_n$ force and flows toward the poles with speeds up to twice the Alfvén speed. In the past, a number of ISEE magnetopause crossings in which such plasma jetting was observed have been interpreted in terms of reconnection, on the basis of a quantitative check of the tangential stress balance across the magnetopause. In this paper, we examine the total energy balance instead for two events (August 9 and September 8, 1978), with the objective of obtaining an additional check on the interpretation in terms of reconnection. The results are: (i) To within experimental uncertainties, the plasma and magnetic field data are consistent with reconnection; (ii) An enthalpy increase comparable to the kinetic energy increase occurs in the magnetopause. Thus substantial dissipation is present in the rotational discontinuity; (iii) During the September 8 event, an ion heat flow associated with a beam of reflected magnetosheath particles carried away some 20% of the total converted electromagnetic energy; (iv) The energy balance provides a persuasive check of the inferred location of the ISEE spacecraft as being south of the reconnection line on August 9, and north of it on September 8.

1. INTRODUCTION

Three recent articles (Paper I: Paschmann, et al., 1979; Paper II: Sonnerup, et al., 1981; Paper III: Gosling, et al., 1982) have contained information on a total of 12 instances of large plasma flow velocities near the magnetopause, observed by the spacecraft ISEE 1 and 2. These observations were interpreted in terms of the magnetic field reconnection process, one of the most striking directly observable effects of which is the generation of high-speed plasma jets directed away from the reconnection site, i.e., away from the so-called X line. It was shown in Papers I-III that, within experimental uncertainties, the observed plasma jet velocities in several of the events was consistent with the reconnection model. In this model, described in detail in Paper II, the jets consist of magnetosheath plasma that has crossed the magnetopause and has been accelerated by the $\underline{I} \times \underline{B}_n$ force there. Here $\underline{I}$ and $\underline{B}_n$ are the current in, and the magnetic field normal to, the magnetopause, respectively, and the magnetopause away from the reconnection line is a rotational discontinuity. Additional support for the interpretation of these events in terms of reconnection has been obtained by examination of energetic particle anisotropies (Scholer, et al., 1981; Paper II) and particle reflection at the magnetopause (Paper II; Scholer and Ipavich, 1983.)

On the other hand, the interpretation of one event (September 8, 1978) in terms of reconnection has been questioned by Eastman and Frank (1982). Further detailed observational information concerning this event may be found in Scholer, et al. (1982) and a possible resolution of the observational dilemma discussed by Eastman and Frank has been proposed by Daly and Fritz (1982).

In addition to the tangential momentum balance, which was studied in Papers I-III, it is also desirable to check the energy budget during these plasma acceleration events. Indeed, Heikkila's (1975) challenge of the magnetopause reconnection model was based on an energy, not a momentum argument. The question is whether the electromagnetic energy, $\underline{E}\cdot\underline{I}$, converted per unit area of the magnetopause during reconnection can be accounted for in terms of the increase in kinetic energy of the magnetosheath plasma as it flows across the magnetopause into the jets, in terms of an increase in the enthalpy of this plasma, and in terms of heat flow away from the magnetopause. It is worth noting that except for heat flow, ohmic and viscous dissipation, the energy conservation law describes reversible thermo- and electromechanical conversion and can be derived directly from the momentum conservation law and the double adiabatic relations. Thus the momentum balance check in Papers I-III automatically provides a partial check of the energy budget.

It is the purpose of this paper to examine the full energy balance at the magnetopause in order to see if a further check can be obtained of the interpretation of the plasma acceleration events in terms of the reconnection model. In Section 2, we review the energy balance equation and cast it in a form suitable for application to the ISEE 1 and 2 plasma and magnetic field observations. The former are obtained from the MPE/LANL fast plasma analyzer, the latter from the UCLA magnetometer onboard the spacecraft. In Section 3 we examine two acceleration events from Paper II (September 8, 1978; August 9, 1978) in detail, and in Section 4 we discuss the results and present our conclusions.

2. ENERGY EQUATION

The steady-state energy balance in a one-dimensional plasma discontinuity may be written in the form

$$\rho(\underline{v}\cdot\underline{n})\Delta\{\tfrac{1}{2}v^2+U\} + \Delta\{\underline{v}\cdot\underline{\underline{P}}\cdot\underline{n}\} + \Delta\{\underline{q}\cdot\underline{n}\} + \Delta\{(\underline{E}\times\underline{B}/\mu_0)\cdot\underline{n}\} = 0 \qquad (1)$$

Here ρ and $\underline{v}$ are the plasma density and velocity, respectively, and $\underline{q}$ is the heat flow vector. Also, $\underline{\underline{P}}$ is the full electron and ion pressure tensor, U is the internal energy per unit mass, and $\underline{E}\times\underline{B}/\mu_0$ is the Poynting vector. The symbol $\Delta\{\ \}$ indicates the change in the quantity in braces from one position of observation to another along the vector $\underline{n}$ normal to the layer. In the present application, $\underline{n}$ is the magnetopause normal and is taken to point outward from the earth. Thus the (constant) mass flux across the layer, $\rho(\underline{v}\cdot\underline{n})$, is negative. In the paper we shall employ a right-handed cartesian coordinate system (x,y,z) with the x axis along $\underline{n}$. The two positions of observation will be a fixed reference point in the magnetosheath near the magnetopause, denoted by the subscript 1, and a movable point in the magnetopause current layer or in the boundary layer inside it, denoted by the subscript 2. With this notation, we have, for example, $\Delta\{U\} = U_2-U_1$.

The first term in Eq. (1) represents the change in kinetic and internal energy as the plasma moves inward through the magnetopause current layer. The internal energy may be written

$$U = (\mathrm{Tr}\underline{\underline{P}})/2\rho = p_{\parallel}/2\rho+p_{\perp}/\rho \qquad (2)$$

where $p_{\parallel}$ and $p_{\perp}$ are the pressures parallel and perpendicular to the magnetic field, respectively. Thus the internal energy, i.e., the sum $(p_{\parallel}/2+p_{\perp})$, can be obtained directly as the trace of a measured pressure tensor but to calculate $p_{\parallel}$ and $p_{\perp}$ individually, certain assumptions are needed concerning the viscous

part of the tensor.

The second term in Eq. (1) is the net rate of work done on the slab of plasma located between points 1 and 2 by the various stress components. It incorporates both the flow work, i.e., the work produced by a diagonal stress tensor with components ($p_{//}$,$p_{\perp}$,$p_{\perp}$), and the work done by the viscous stresses acting on the surfaces of the slab. If we denote the latter by $\rho(\underline{v}\cdot\underline{n})\Delta\{W\}$ we may then demonstrate that

$$\Delta\{\underline{v}\cdot\underline{\underline{P}}\cdot\underline{n}\} = \rho(\underline{v}\cdot\underline{n})\Delta\{p_{\perp}/\rho\} + (\underline{B}\cdot\underline{n})\Delta\{\alpha(\underline{v}\cdot\underline{B})/\mu_0\} + \rho(\underline{v}\cdot\underline{n})\Delta\{W\} \qquad (3)$$

where α is the anisotropy factor, i.e., $\alpha \equiv (p_{//} - p_{\perp})\mu_0/B^2$. The rate of work done by viscous stresses at station 1 is zero, i.e, $W_1 = 0$, since this point is located outside the region of velocity shear. This is also true for station 2, $W_2 = 0$, when this point is located in a uniform plasma region inside the magnetopause. In that case, no viscous term remains. But if station 2 is located in a region of high velocity shear in the magnetopause a substantial viscous contribution could be present. It is difficult to estimate the magnitude of this contribution but it should be possible to determine its sign by use of the regular expression for the viscous stress tensor in a newtonian fluid with viscosity μ. The result is

$$\rho(\underline{v}\cdot\underline{n})W_2 = -\mu_2\left[\frac{d}{dx}\,(v_y^2/2+v_z^2/2+2v_x^2/3)\right]_2 \qquad (4)$$

During these events, the tangential velocity components v_y and v_z in the magnetopause are much larger than v_x and they decrease with increasing x. In other words, the right hand side of Eq. (4) is positive. Since $(\underline{v}\cdot\underline{n})<0$, we therefore conclude that W_2 is negative in the magnetopause.

It is convenient to write the third term in Eq. (1) in the form

$$\Delta\{\underline{q}\cdot\underline{n}\} = \rho(\underline{v}\cdot\underline{n})Q \qquad (5)$$

where Q represents the net ion and electron heat flow per unit mass away from the plasma slab located between points 1 and 2. It is difficult to predict the magnitude of Q theoretically but since the magnetopause and boundary layer plasma appears to be heated one would expect a net heat flow away from the entire region, i.e., $Q \geq 0$. Furthermore it can be argued that Q should be smaller the closer point 2 is to point 1. We shall show from the observations that this term sometimes makes an important contribution to the energy balance.

Finally, the fourth term in Eq. (1) is the net transport of electromagnetic energy into the region between stations 1 and 2. Since the tangential component of the electric field remains constant in the layer and since the change in tangential magnetic field is proportional to the total electric current $\underline{I}_{21}$ in the slab between stations 1 and 2, this term may also be written in the familiar form $\underline{E}\cdot\underline{I}_{21}$.

If we write Ohm's law as

$$\underline{E} + \underline{v} \times \underline{B} = \underline{\eta}\cdot\underline{j} \tag{6}$$

where $\underline{\eta}$ is an effective resistivity tensor and $\underline{j}$ the current density, we may transform the fourth term in Eq. (1) to the following form:

$$\Delta\{(\underline{E}\times\underline{B})\cdot\underline{n}/\mu_0\} = \Delta\{-[(\underline{v}\times\underline{B})\times\underline{B}]\cdot\underline{n}/\mu_0\} + \Delta\{[(\underline{\eta}\cdot\underline{j})\times\underline{B}]\cdot\underline{n}/\mu_0\} \tag{7}$$

The right-hand side may be further rewritten by expansion of the vector triple product in the first term:

$$\Delta\{(\underline{E}\times\underline{B})\cdot\underline{n}/\mu_0\} = \Delta\{(\underline{v}\cdot\underline{n})(B^2/\mu_0)-(\underline{B}\cdot\underline{n})(\underline{v}\cdot\underline{B})/\mu_0\} + \rho(\underline{v}\cdot\underline{n})\Delta\{R\} \tag{8}$$

where the last term on the right represents the resistive contribution in Eq. (7). The quantity R_1 vanishes at station 1 where $\underline{j}=0$, i.e., $R_1=0$. It

also vanishes at station 2, $R_2=0$, except when this point is located in the magnetopause itself where $\underline{j}$ is large. It is difficult to produce a reliable theoretical estimate of $\underline{\eta}$ but, for illustrative purposes, we may assume a scalar resistivity η in which case the resistive term reduces to

$$\rho(\underline{v}\cdot\underline{n})\Delta\{R\} = \Delta\{-\eta\underline{n}\cdot\underline{\nabla}B^2/2\mu_0^2\} \tag{9}$$

or

$$\rho(\underline{v}\cdot\underline{n})R_2 = -\eta_2\underline{n}\cdot\underline{\nabla}B_2^2/2\mu_0^2 \tag{10}$$

Since the magnetic pressure usually has a minimum in the magnetopause (and since $(\underline{v}\cdot\underline{n})<0$), we expect $R_2>0$ in the outer half of the magnetopause structure and $R_2<0$ in the inner half.

If Eq. (1) is divided by the (negative and constant) mass flux $\rho(\underline{v}\cdot\underline{n})$ and the expressions (2), (3), (5), and (8) are used for the individual terms, we obtain

$$\underset{①}{\Delta\left\{\frac{v^2}{2}\right\}} + \underset{②}{\Delta\left\{\frac{5}{2}\frac{p_\perp}{\rho}\right\}} + W_2 + Q = \underset{③}{\Delta\left\{-\left(1+\frac{\alpha}{2}\right)\frac{B^2}{\mu_0\rho}\right\}} + \underset{④}{\Delta\left\{\frac{(1-\alpha)(\underline{B}\cdot\underline{n})}{\rho_1(\underline{v}_1\cdot\underline{n})\mu_0}(\underline{v}\cdot\underline{B})\right\}} - R_2 \tag{11}$$

In term ④, $(\underline{v}_1\cdot\underline{n})$ may be replaced by the Alfvén speed $\pm(\underline{B}\cdot\underline{n})\sqrt{(1-\alpha_1)/\mu_0\rho_1}$ as is appropriate for a rotational discontinuity. The upper sign applies north of the reconnection line in the standard reconnection model where $\underline{B}\cdot\underline{n}<0$, and the lower sign south of that line where $\underline{B}\cdot\underline{n}>0$.

In summary, for isotropic pressure, $\alpha=0$, terms ① and ② in Eq. (11) represent the increase in kinetic energy and enthalpy per unit mass of the plasma as it moves from station 1 to station 2 while terms ③ and ④ represent the nonresistive part of the electromagnetic energy input. For nonisotropic pressure, $\alpha\neq0$, some of the terms contributing to the enthalpy appear on the right-hand side of Eq. (11). Also, the term Q is the net heat

flow and is expected to be positive or zero; W_2 is the viscous contribution at station 2 and is expected to be negative in the magnetopause and approximately zero in the boundary layer plasma; R_2 is the resistive contribution and is expected to be positive in the outer half of the magnetopause, negative in the inner half, and zero in the boundary layer.

Except as noted below, the terms ①-④ in Eq. (11) are directly measured on ISEE 1 and 2 and will form the basis for our check of the energy balance. Apart from small viscous corrections, the perpendicular pressure, $p_\perp$, is usually reasonably well determined by the MPE/LANL fast plasma analyzer throughout the magnetopause and boundary layer. On the other hand, the parallel pressure, $p_{\parallel}$, is well determined only on the magnetosheath side of the magnetopause where the magnetic field usually lies near the spacecraft equatorial plane. On the magnetospheric side, the magnetic field orientation falls in the blind direction of the instrument along the spacecraft spin axis. Thus α_1, but not α_2, is measured directly. However, α_2 can be inferred from the measured densities by use of the relation $\rho_1(1-\alpha_1) = \rho_2(1-\alpha_2)$ which applies across a rotational discontinuity. This procedure was also employed in Paper II. It is not strictly justified when station 2 lies in the magnetopause. For this and other reasons it may occasionally yield unphysical results: if the inferred α_2 value is large and negative while at the same time the measured ratio $p_{\perp 2}\mu_0/B_2^2$ is small then the formula $\alpha_2 = (p_{\parallel 2}-P_{\perp 2})\mu_0/B_2^2$ will lead to a negative value for $p_{\parallel 2}$. Such points have been eliminated.

3. OBSERVATIONS

September 8, 1978: Detailed information concerning this high-speed flow event may be found in Papers I and II. For purposes of review, the first three panels of Fig. 1 show the plasma density, the GSM Z component of the magnetic field, and the field magnitude, measured by ISEE 1 during its outward passage through the magnetopause region. The principal magnetopause crossing is indicated by the reversal of B_Z at 00.44 UT. It is followed by a partial reentry of the spacecraft in the interval 00.46 - 00.51 UT which resulted from an outward-inward motion of the magnetopause. The bottom panels of Fig. 1 show the kinetic energy $v^2/2$ and the enthalpy $(5/2)p/\rho = (5/2)kT/m$ where $p = (p_{\parallel} + 2p_{\perp})/3$. The high-speed flow regions in the magnetopause and boundary layer are clearly seen. It is also observed that the high-speed plasma was much hotter than the ambient plasma. On the average, the enthalpy increase was comparable to, but somewhat smaller than, the kinetic energy increase. The ISEE 2 data for this event are not shown but they have the same qualitative properties as the ISEE 1 data and they will be used below. As discussed in Paper II, ISEE 2 experienced only a single crossing of the magnetopause during part of which a data gap occurred.

In order to check the validity of the energy equation (11) we now apply that equation between the reference point 1 in the magnetosheath adjacent to the magnetopause and those individual measurements at a point 2 in or inside the magnetopause which meet the selection criteria described in detail in the appendix of Paper II. The reference values are averages over several measurements.

Figure 2 shows a scatter diagram of the terms $\Delta\{①+②\}$ versus $\Delta\{③+④\}$, i.e., approximately, of the kinetic energy and enthalpy increase versus the electromagnetic energy supplied. In order to illustrate that the

effect of the α terms is relatively small, we have shown terms (3) and (4) both with the measured α_1 values and with $\alpha_1 = 0$. In both cases α_2 is determined from the density ratio ρ_1/ρ_2 as described earlier.

If the ideal reconnection model applies, then, in the absence of Q, W_2, R_2, and experimental uncertainties, the data in Fig. 2 should fall along the 45° line. The figure shows that the data from the main ISEE 1 crossing and from the ISEE 2 crossing fall mainly below the line whereas the data from the partial ISEE 1 crossing fall above it. This effect may be systematic and, if so, we believe it can be explained qualitatively by our neglect of the terms Q and W_2, as described below.

Data from the main ISEE 1 crossing and from the ISEE 2 crossing have station 2 located mainly in the boundary layer or in the innermost part of the magnetopause. As pointed out in Section 2, for this situation one expects that the net heat flow Q away from the magnetopause could be substantial (Q>0) while the viscous work W_2 and the resistive term R_2 are both small. The expected net result is that the data points should fall below the 45° line in Fig. 2 as indeed they do. A quantitative estimate of Q, based on observed fluxes of reflected magnetosheath ions, will be given in the discussion section.

Data from the partial ISEE 1 crossing have station 2 located mostly in the outer half of the magnetopause. In this case, the net heat flow Q may be small and the negative W_2 term may provide the largest correction. Neglect of this term causes the data points in Fig. 2 to fall above the 45° line as indeed they do. In the discussion section, we shall estimate W_2 and R_2 and show that W_2 may be substantial while R_2 (which would move the data points in Fig. 2 to the left) is probably small.

In Fig. 2, the sign chosen for term ④ corresponds to a crossing north of the reconnection line since that was the location deduced in Papers I and II. Reversal of the sign of this term moves all points in Fig. 2 to the left as shown in Fig. 3. Such a shift would destroy the rough overall agreement of the data with the 45° line. Thus the energy balance supports the identification of this case as a crossing north of the reconnection line.

August 9, 1978: The format of the data presentation is the same as in the previous case. As shown in Fig. 4, the data used for this event correspond to a partial crossing of the magnetopause during the interval 19.34 - 19.53 UT. During the rapid main crossing, at 20.10 UT no plasma acceleration was measured. It appears that an abrupt change in the magnetosheath conditions may have caused the density change at 19.53 UT at the end of the partial crossing. For this reason, the data for the reference point 1 was formed as an average over magnetosheath measurements immediately preceding the event. The increases in plasma kinetic energy and enthalpy were smaller than in the September 8, 1978, event and, on the average, the latter increase somewhat exceeded the former.

Figure 5 shows the terms $\Delta\{①+②\}$ versus $\Delta\{③+④\}$ for the August 9 event (for ISEE 1 and 2). All of the data points are seen to fall above the 45° line. This behavior is consistent with our expectation for data from partial magnetopause crossings where station 2 is located in the magnetopause so that $W_2<0$. If this term were included, the data points in Fig. 4 would move down towards the 45° line. For this event there was no clear evidence of reflected magnetosheath ions so that the ion heat flow away from the magnetopause was presumably small. And the R_2 term should be small because $\underline{\nabla}B_2^2$ is small.

In Fig. 5 the sign of term ④ chosen corresponds to a crossing south of the reconnection line since that was the location deduced in Paper II. The opposite choice of sign is made in Fig. 6, in which most of the points are seen to have negative values of the abscissa. It would be difficult to argue that the data in this figure have an tendency to agree with the 45° line. Thus the energy balance supports the identification of this case as a crossing south of the reconnection line.

4. DISCUSSION

Figure 2 shows that the data points from the complete magnetopause crossings by ISEE 1 and ISEE 2 on September 8, 1978, fall systematically below the 45° line. In other words, these data indicate that all of the electromagnetic energy dissipated in the magnetopause does not show up as kinetic energy and enthalpy imparted to the plasma as it crosses this current layer. We shall now show that most of the missing energy leaves the system in the form of heat flow associated with a population of magnetosheath ions which is reflected and energized at the magnetopause and returns upstream as a beam flowing nearly along the magnetic field. As reported in Paper II, this beam has a density of approximately 20% of the magnetosheath density and a velocity of about 500 km/s. It is easy to show that the heat flow vector in a plasma consisting of two cold ion beams, of density $r\rho_1$ and $(1-r)\rho_1$, having velocity difference $\underline{\Delta v}$, is

$$\underline{q}_1 = \tfrac{1}{2}\rho_1 r(1-r)(1-2r)|\underline{\Delta v}|^2\underline{\Delta v}$$

where in the present case $\underline{\Delta v} \simeq -|\underline{\Delta v}|\underline{B}_1/|B_1|$. From Eq. (5) with $\underline{q}_2=0$ and $(\underline{v}_1\cdot\underline{n}) = (\underline{B}\cdot\underline{n})\sqrt{(1-\alpha_1)/\mu_0\rho_1}$ we then find

$$Q = -\frac{(\underline{q}_1\cdot\underline{n})}{\rho_1(\underline{v}_1\cdot\underline{n})} = \tfrac{1}{2}r(1-r)(1-2r)|\underline{\Delta v}|^3/v_{A1}$$

where $v_{A1} = |\underline{B}_1|\sqrt{(1-\alpha_1)/\mu_0\rho_1}$. For $r \simeq 0.2$, $|\underline{\Delta v}| \simeq 500$ km/s and $v_{A1} = 300$ km/s we find $Q = 2\times10^{14}\text{cm}^2/\text{s}^2$. Values of Q of this order of magnitude are also obtained by direct integration over the measured ion distribution function.

If the data points for the two complete magnetopause crossings in Fig. 2 are moved upwards by $2\times10^{14}\text{cm}^2/\text{s}^2$ then, on the average, their location will coincide well with the 45° line. The remaining discrepancy may be easily

accounted for in terms of the uncertainties in the measurements.

It is more difficult to provide reliable estimates of the terms W_2 and R_2 which, as we have argued, tend to move data points in Figs. 2 and 4 from the partial crossings downwards and to the left. However, we may write these terms as

$$W_2 \simeq D_v \frac{(\Delta v)^2}{h(\underline{v}\cdot\underline{n})}$$

$$R_2 \simeq D_n \frac{(\Delta v_A)^2}{h(\underline{v}\cdot\underline{n})}$$

where h is the magnetopause thickness and Δv^2 and Δv_A^2 are characteristic changes of flow speed and Alfvén speed in the magnetopause. Also D_v and D_n are the viscous (μ/ρ) and resistive (η/μ_o) diffusion coefficients, respectively. As an example, for the September 8 event, we may choose Δv = 400 km/s, Δv_A = 150 km/s, h = 100 km, and $(\underline{v}\cdot\underline{n})$ = 30 km/s. In order to produce a value of $3\times10^{14}cm^2/s^2$ for W_2 or R_2, which is of the order of the corrections needed (see Fig. 2), the diffusion coefficients would have to be $D_v \sim 5\times10^{12}cm^2/s$ and $D_n \sim 4\times10^{13}cm^2/s$. These values should be compared to the diffusion coefficient $D = R_g^2/T_g$ corresponding to a diffusion speed of one gyro radius R_g per ion gyroperiod T_g. For $R_g \sim 50$ km and $T_g \sim 1$s we have $D = 2.5\times10^{13}cm^2/s$. Comparison with D now indicates that the above value for D_v is reasonable while that for D_n is too large. Thus we expect the dominant correction term to be W_2. With reasonable assumptions, this term can become sufficiently large to move the data points for the partial crossings down to the 45° line in Fig. 2.

For the August 9 event, the quantity $(\underline{v}\cdot\underline{n})$ is not known. Therefore it becomes impossible to produce reliable estimates of the required diffusion coefficients. However the magnetic field magnitude change was small during the crossing so that the correction term R_2 was probably small in this case also.

In summary, our examination of the energy balance during two plasma acceleration events (September 8 and August 9, 1978) has led to the following results:

(i) To within experimental and other uncertainties the data are consistent with the interpretation in terms of magnetic field reconnection offered in Papers I and II. This consistency includes an explicit check on the sign of the magnetic field component normal to the magnetopause.

(ii) The enthalpy increase of the magnetosheath plasma as it crosses the magnetopause during reconnection is substantial and is comparable to its increase in kinetic energy.

(iii) During the September 8 event, a substantial ion heat flow from the magnetopause outward into the magnetosheath was present. This heat flow carries away some 20% of the total electromagnetic energy dissipated in the magnetopause.

(iv) In the magnetopause structure itself, the energy budget may include substantial contributions from viscous effects.

The experimental uncertainties involved in this examination of the energy budget are large. And, as emphasized in Paper II, the theoretical model to which the data are compared is undoubtedly oversimplified in many respects. Nevertheless, in our view, the results reported here add substantial support to the interpretation of these two plasma acceleration events in terms of the magnetic field reconnection process. We have also established that the energy conversion in the magnetopause during reconnection is not purely electromechanical. A substantial amount of dissipation occurs and produces heating of the plasma as it crosses the current layer. Such behavior, while perhaps unexpected, is nevertheless entirely consistent with

the jump conditions across rotational discontinuities in a plasma with nonisotropic pressure (Hudson, 1970; 1971; 1973).

Acknowledgement: Research at Dartmouth College was supported by the National Aeronautics and Space Administration under grant NSG5348 and by the National Science Foundation, Atmospheric Sciences Division under grant ATM-8201974.

REFERENCES

Daly, P.W., and T.A. Fritz, Trapped electron distributions on open magnetic field lines, J. Geophys. Res., 87, 6081-6088, 1982.

Eastman, T.E., and L.A. Frank, Observations of high-speed plasma flow near the earth's magnetopause: evidence for reconnection, J. Geophys. Res., 87, 2187-2201, 1982.

Gosling, J.T., J.R. Asbridge, S.J. Bame, W.C. Feldman, G. Paschmann, N. Sckopke, and C.T. Russell, Evidence for quasi-steady reconnection at the dayside magnetopause, J. Geophys. Res., 87, 2147-2158, 1982.

Heikkila, W.J., Is there an electrostatic field tangential to the dayside magnetopause and neutral line?, Geophys. Res. Lett., 2, 154-157, 1975.

Hudson, P.D., Discontinuities in an anisotropic plasma and their identification in the solar wind, Planet. Space Sci., 18, 1611-1622, 1970.

Hudson, P.D., Rotational discontinuities in an anisotropic plasma, Planet. Space Sci., 19, 1693-1699, 1971.

Hudson, P.D., Rotational discontinuities in an anisotropic plasma-II, Planet. Space Sci., 21, 475-483, 1973.

Paschmann, G., B.U.Ö. Sonnerup, I. Papamastorakis, N. Sckopke, G. Haerendel, S.J. Bame, J.R. Asbridge, J.T. Gosling, C.T. Russell, and R.C. Elphic, Plasma acceleration at the earth's magnetopause: Evidence for reconnection, Nature, 282, 243-246, 1979.

Scholer, M., F.M. Ipavich, G. Gloeckler, D. Hovestadt, and B. Klecker, Leakage of magnetospheric ions into the magnetosheath along reconnected field lines at the dayside magnetopause, J. Geophys. Res., 86, 1299-1304, 1981.

Scholer, M., P.W. Daly, G. Paschmann, and T.A. Fritz, Field-line topology determined by energetic particles during a possible magnetopause reconnection event, J. Geophys. Res., 87, 6073-6080, 1982.

Scholer, M., and F.M. Ipavich, Interaction of ring current ions with the magnetopause, J. Geophys. Res., 88, 6937-6943, 1983.

Sonnerup, B.U.Ö., G. Paschmann, I. Papamastorakis, N. Sckopke, G. Haerendel, S.J. Bame, J.R. Asbridge, J.T. Gosling, and C.T. Russell, Evidence for magnetic field reconnection at the earth's magnetopause, J. Geophys. Res., 86, 10,049-10,067, 1981.

FIGURE CAPTIONS

Fig. 1 Plasma and magnetic field data from ISEE 1 for a 36-min. interval on September 8, 1978. From the top, the panels show: the plasma density N_p; the GSM Z component of the magnetic field B_Z; the field magnitude B; the kinetic energy $v^2/2$ and the enthalpy $5kT/2m$, per unit mass (both in units of $10^{14}cm^2/s^2$). Note the high values of the latter two quantities in the magnetopause (MP) and boundary layer (BL) regions. Heating in the magnetosheath adjacent to the magnetopause is also evident.

Fig. 2 Scatter plot of terms ① and ② versus terms ③ and ④ in the energy balance equation (11) for the September 8, 1978, event. The sign of term ④ corresponds to a crossing north of the reconnection line ($B_n<0$). The symbols (+) and (·) denote the principal magnetopause crossing by ISEE 1 and the only crossing by ISEE 2, respectively. The symbols (X) and (0) denote the left-hand and right-hand halves of the partial ISEE 1 crossing. Bars extending from these symbols indicate the change in the location of data points if one puts $\alpha_1=0$.

Fig. 3 Same as Fig. 2 but with the opposite sign of term ④.

Fig. 4 Plasma and magnetic field data from ISEE 1 for a 60-min. interval on August 9, 1978. See Fig. 1.

Fig. 5 Scatter plot of terms ① and ② versus terms ③ and ④ in the energy balance equation (11) for the August 9, 1978, event. The sign of term ④ corresponds to a crossing south of the reconnection line ($B_n>0$).

Fig. 6 Same as Fig. 5 but with the opposite sign of term ④.

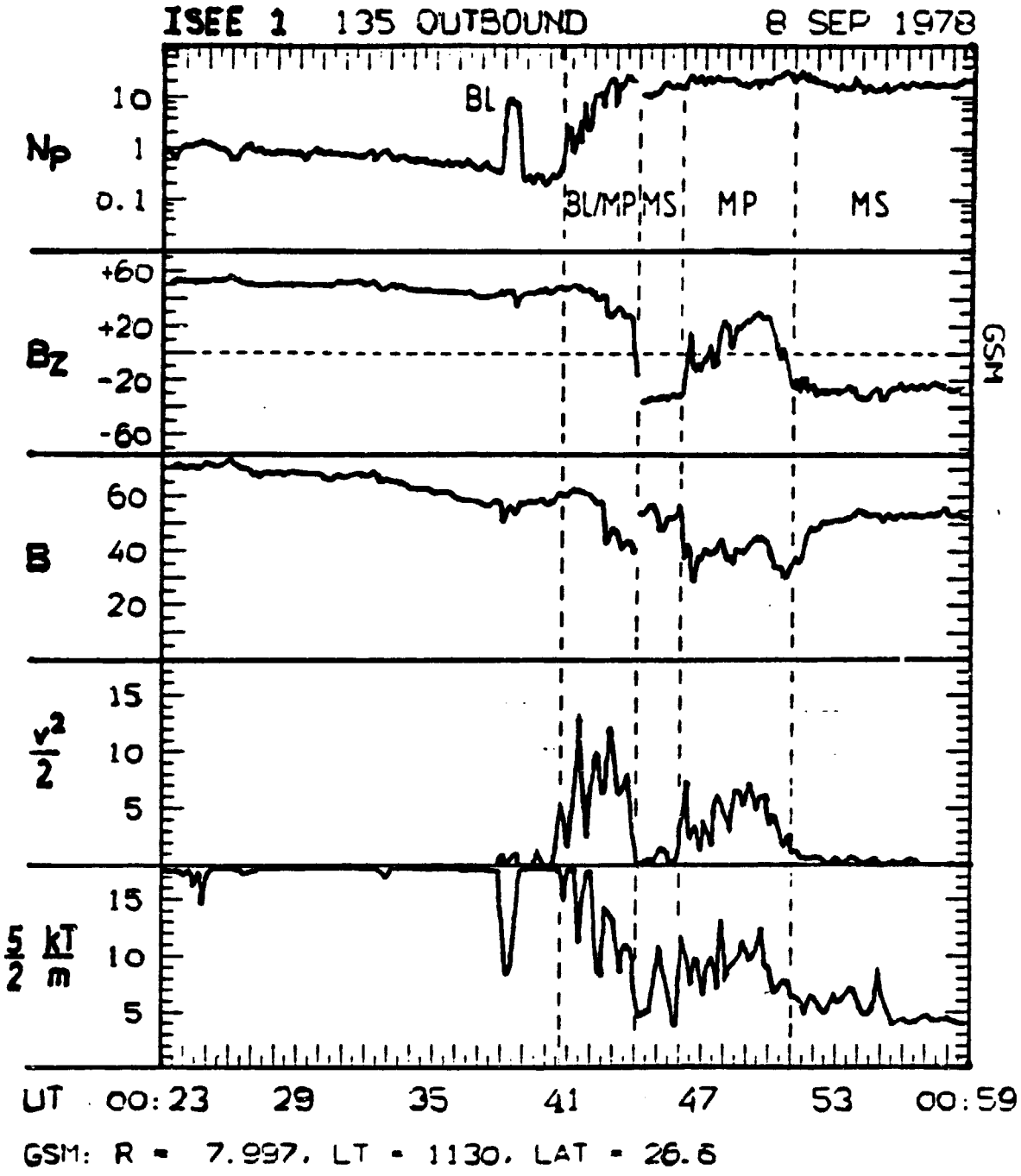

Figure 1

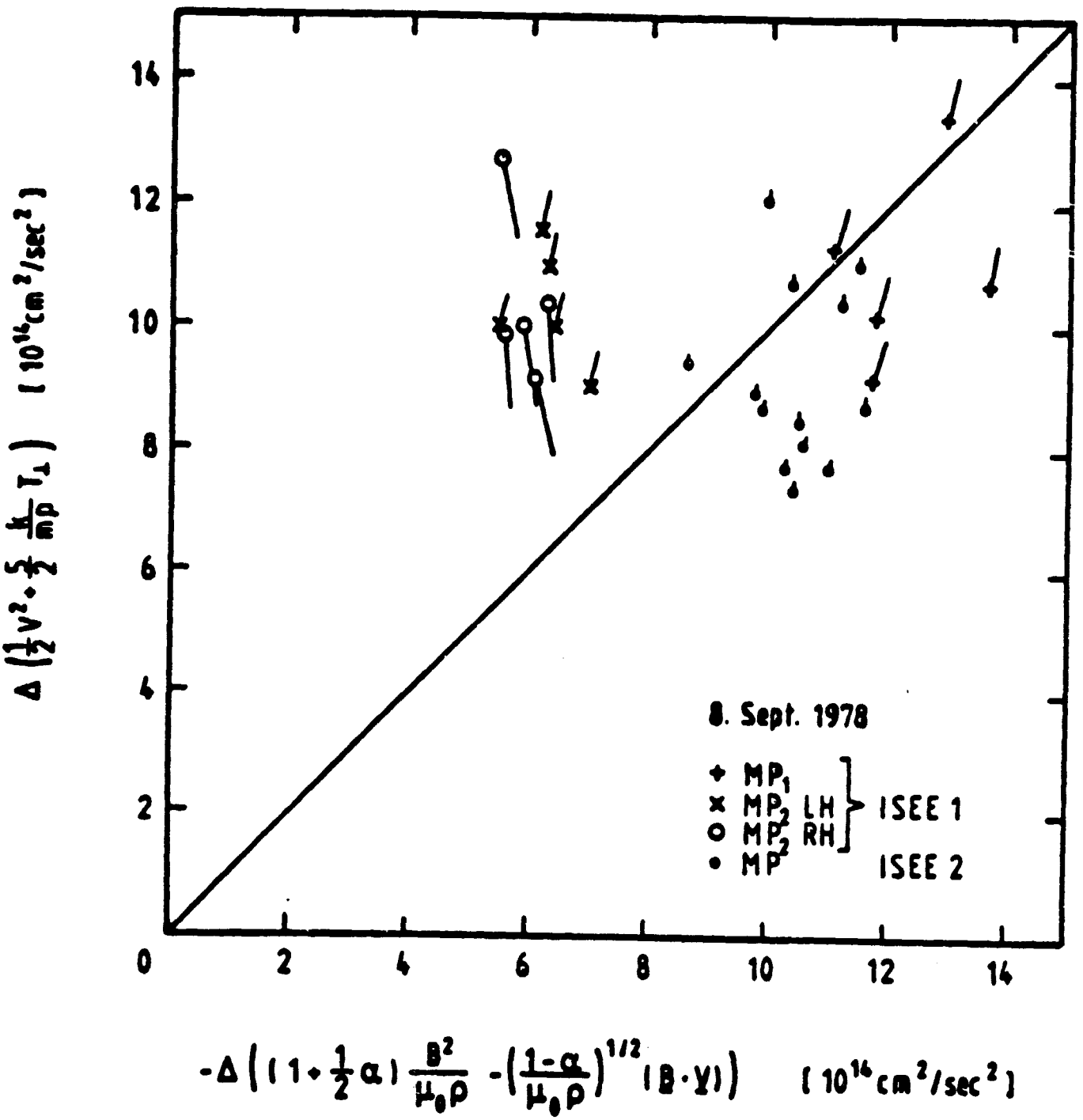

Figure 2

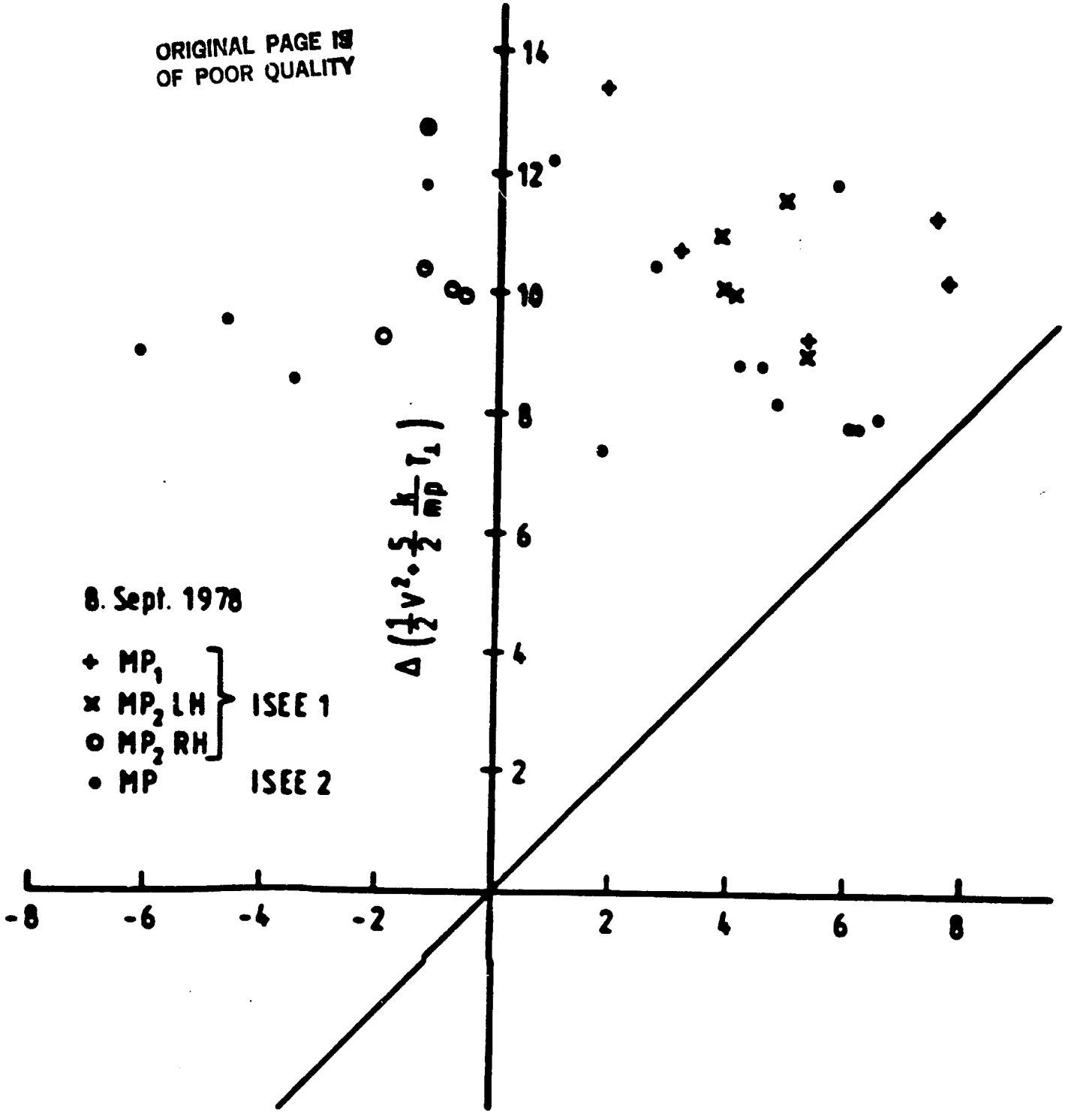

Figure 3

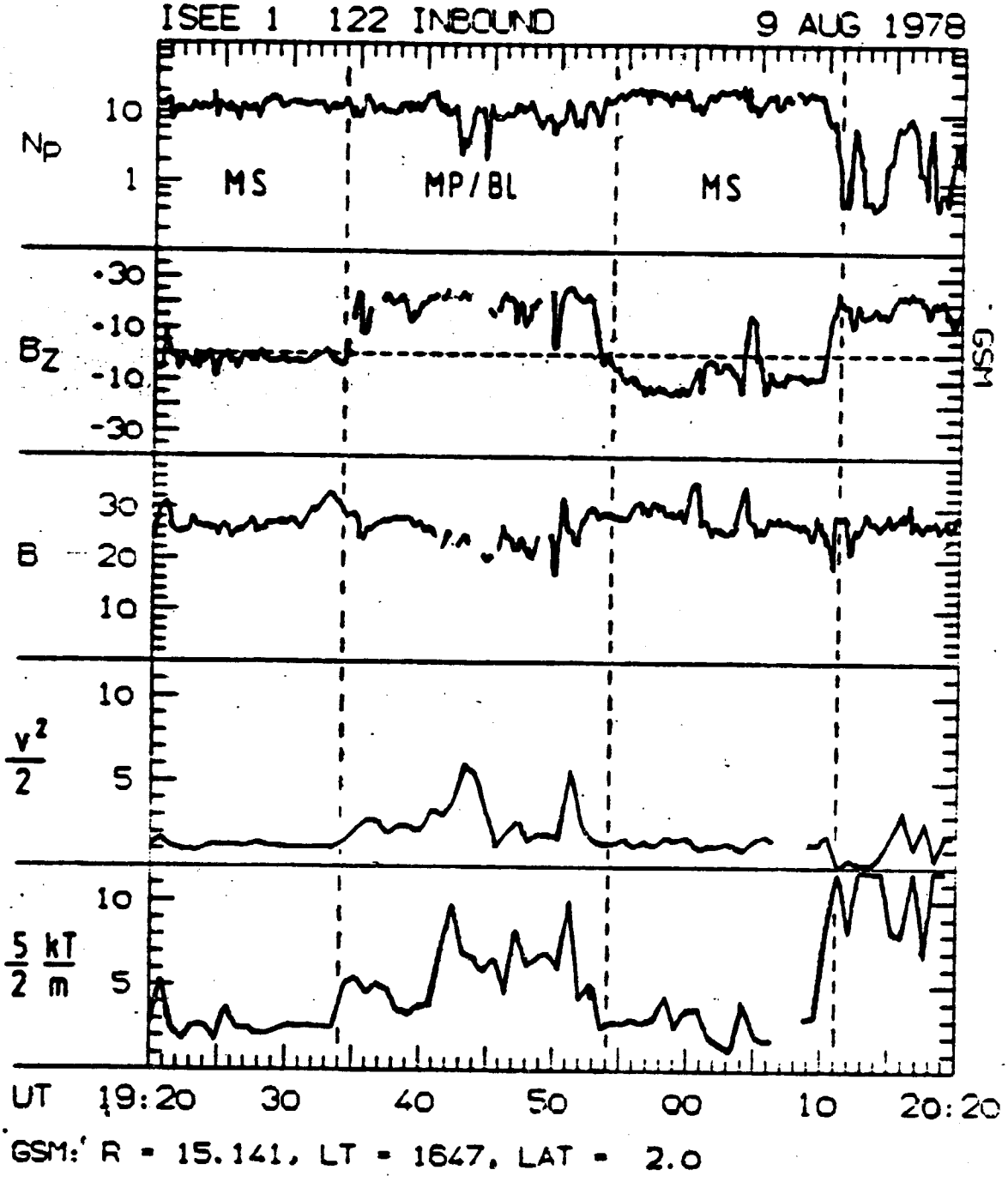

Figure 4

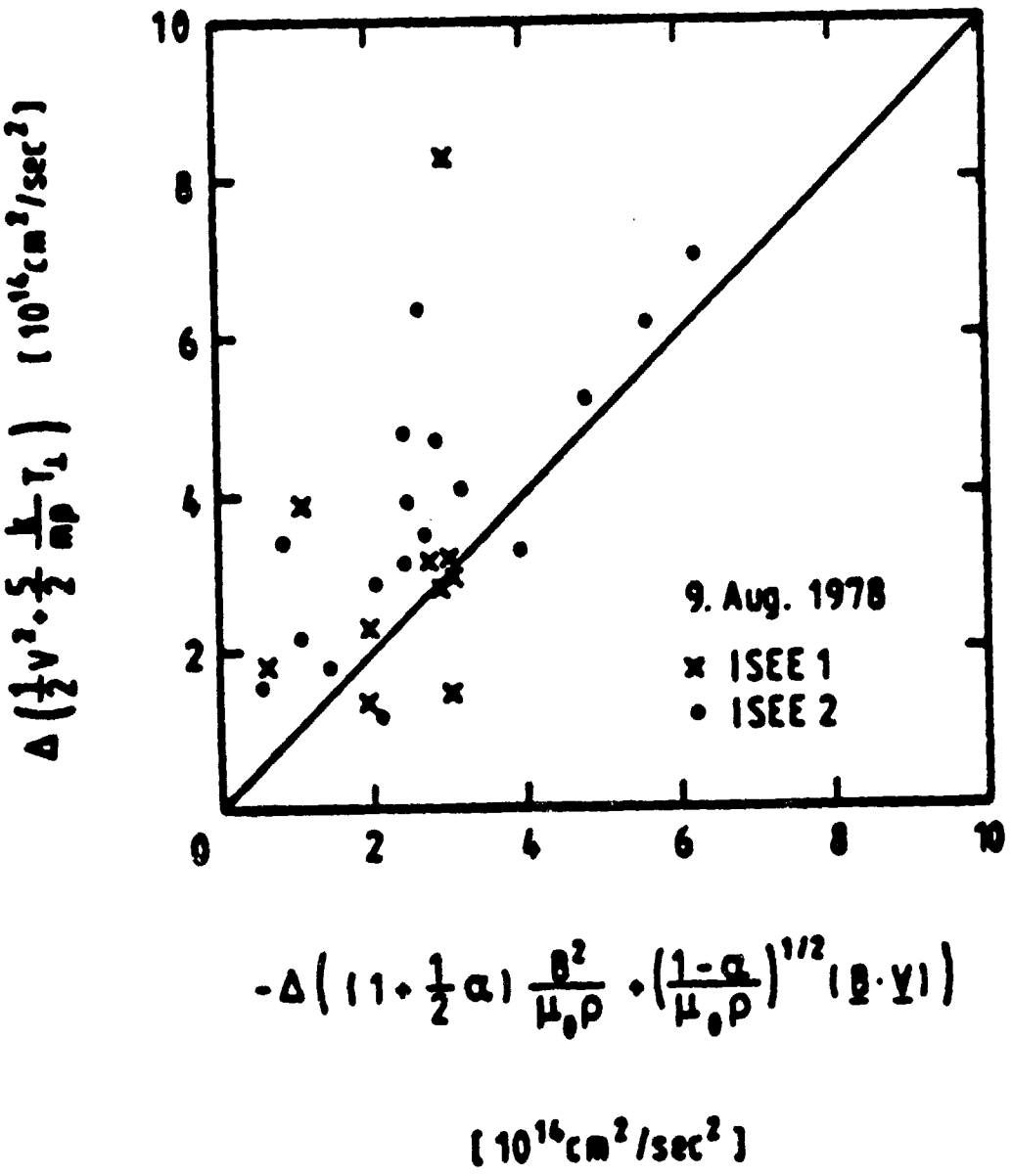

Figure 5

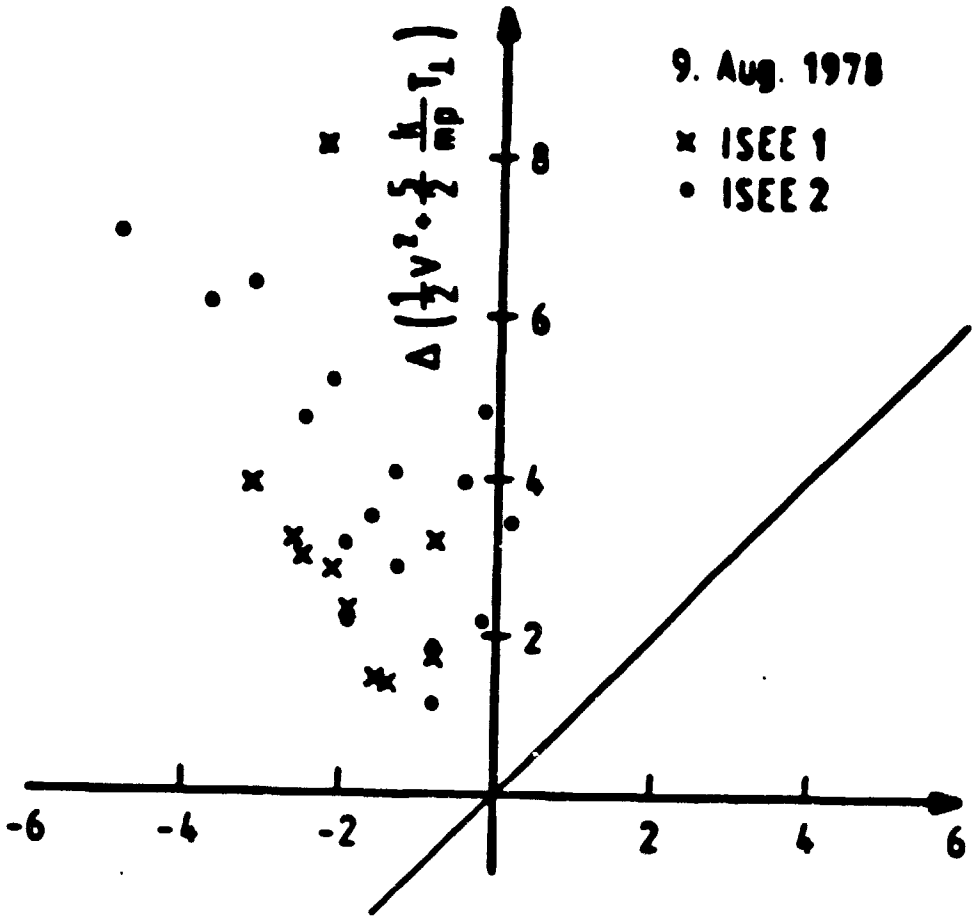

Figure 6

OMIT
TO
END

An Analytic Model of Current Layers in a Collision-Free Plasma With Anisotropic Pressure

Keith B. Kirkland
M.S. Thesis
September 1980

Abstract

In any ionized gas, or plasma, with an imbedded magnetic field, an abrupt change in the orientation and strength of the field at a surface implies the existence of a thin sheet of current at that location. Such current sheets provide boundaries between different magnetic domain and are common in the solar system. For example, they are found in solar flares and in planetary "bow shocks" and magnetopauses (which occur where the solar wind blows magnetic field lines and plasma of solar origin past planetary magnetic fields). Furthermore, under certain conditions, ions moving in the current sheets may be accelerated to very high energies. Such acceleration occurs sporadically during solar flares and geomagnetic storms.

Current sheets may be divided into four categories: shocks, tangential, rotational, and contact discontinuities. Analytic solutions describing the detailed self-consistent behavior of the magnetic field and the charged particles have been sought for current sheets with a nonvanishing normal magnetic-field component in a collisionless plasma. Tangential discontinuities, which have no normal components, have not been dealt with. In the cold plasma limit, analytic models to date have assumed the plasma to consist of a single beam of cold ions and an accompanying cold electron beam, implying vanishing plasma pressure. This leads to solutions for shock solitons (for which, conditions are identical on the two sides of the layer) but not to rotational or contact discontinuities.

In this thesis, in order to include finite pressure effects, two cold ion beams with different energy were used. The resulting plasma has a finite pressure along the magnetic field but no pressure across it. With this modification, solutions for contact discontinuities were found and rotational discontinuities appear to be possible as well as shock solitons. Particular attention was paid to a class of contact discontinuities for which the magnetic field is coplanar, i.e., it is confined to a plane normal to the current layer. Among these solutions, four subclasses were found: (i) soliton-like layers in which the magnetic field and plasma are identical on the two sides; (ii) periodic solutions consisting of an infinite array of current layers; (iii) reflection layers, in which the incident ion beam is reflected; (iv) trapped layers, where the ions are trapped within the sheet. Finally, the ground has been prepared for exploration of contact discontinuities where B is not coplanar, rotational discontinuities and shock solitons.

A Stability Analysis of the Interface Between the Magnetopause Boundary Layer and the Magnetosphere Including Coupling to the Ionosphere

Susan E. Minas
M.S. Thesis
September 1981

Abstract

The sun is constantly emitting a flux of charged particles, or plasma, known as the solar wind, which flows out into the solar system and past the earth. The magnetic field of the earth carves out a cavity, referred to as the magnetosphere in this flow. Some of the flowing plasma makes it across the cavity boundary, called the magnetopause, and continues to flow in the general direction of the solar wind, in a thin boundary layer.

The plasma flowing in the boundary layer moves across the magnetic field lines of the earth, setting up a natural MHD generator. It is convenient to consider this generator to be hooked up to the resistive auroral ionosphere, with the magnetic field lines acting like wires. Phenomena occurring in the boundary layer are expected to have noticeable effects in the auroral region.

It is known from fluid mechanics that the interface between a flowing and a stationary fluid is susceptible to the Kelvin-Helmholtz (K-H) instability. This is true for a plasma interface as well with the additional feature that any shear in the magnetic field at the interface tends to suppress the instability.

A region of the low latitude boundary layer (LLBL), on the morning side of the earth, within a distance H from the equatorial plane is modeled as an MHD generator for the ionospheric load. In the case of perfect coupling to the ionosphere, magnetic field lines are assumed to be equipotentials and any potential developed across the boundary layer is impressed on the ionosphere, causing a current to flow there which becomes part of a current loop. This current flows across the LLBL and into and out of both the LLBL and ionosphere along magnetic field lines. Perturbations in the field aligned current due to electric field perturbations felt in the ionosphere are matched to the perturbation current in the LLBL associated with perturbations in the magnetic field there. All perturbations are expressed as series expansions in Z, the distance from the equatorial plane, and the dispersion relation is arrived at keeping terms to lowest significant order in Z.

The dispersion relation to this order indicates that the coupling to the ionosphere decreases the growth rate of the instability. It does not exhibit any threshold in flow speed below which the interface is stable. Using observed values for the model parameters it is shown that the growth rate remains sufficiently large so that large amplitude waves would develop during the time required for the K-H waves to travel from the subsolar point to an observation site in the morningside boundary layer. Thus, it seems reasonable to believe that the Kelvin-Helmholtz instability at this interface is responsible for the observed modulation in boundary layer thickness.

A brief summary is given of the steps needed to carry the Z expansion to the next order.

Spectral Analysis of Magnetic Fields Around the Earth's Magnetopause

Fernando Fonseca
M.S. Thesis
December 1983

Abstract

Spectral analysis was performed on magnetic field data obtained near the earth's magnetopause by the fluxgate magnetometers onboard the satellites in the International Sun-Earth Explorer mission (ISEE). Data were analyzed from the plasma boundary layer just inside the magnetopause as well as from the adjoining regions of the magnetosphere and the magnetosheath. A survey of the techniques available to analyze many short segments of data was performed and the most appropriate methods were selected and implemented. The analysis was performed in the frequency range .1 to 1 hertz. Variations in the power spectra of the magnetic field fluctuations of the form f^{-2} were found in the magnetosheath and in the boundary layer. Study of the spectral matrices indicated that the noise in these regions has a propagation direction approximately along the magnetic field and may be associated with the whistler mode. In the magnetosphere a power spectrum of the form f^{-3} was obtained. Except for a small peak at the satellite spin frequency observed in the magnetosphere, no signficant peaks were found in the power spectra from any of the three regions.